Republic of Iraq
Ministry of Higher Education
and Scientific Research
University of Babylon
Faculty of Materials Engineering
Department of Metallurgical Engineering

Studying the Effect of Electrode Type on the Microstructure and Mechanical Properties of Shielded Metal Arc AISI 5155 Low Alloy Steel Welds

A Dissertation

Submitted to the Council of the Faculty of Materials Engineering/University of Babylon in Partial Fulfillment of the Requirements for the Degree of Higher Diploma in Materials Engineering/Metallurgical Engineering.

By

Noor Abd Ali Kadhim Abid

Supervised by Assist. Prof. Abdulsameea J. Al-Kilabi (Ph.D)

2021A.M **1442 A.H**

وَيَسْأَلُونَكَ عَنِ الرُّوحِ قُلِ الرُّوحُ مِنْ أَمْرِ رَبِّي وَمَا أُوتِيتُمْ مِنَ الْعِلْمِ إِلَّا قَلِيلًا

صدق الله العلي العظيم

[سورة الإسراء / آية 85]

Dedication

To the memory of my beloved mother, who never saw this adventure. You are gone but your love, prayers and belief in me has made this journey possible.

To my wonderful father; the origin of my success.

To my husband 'Ali' who has been a source of patience, strength, support and motivation for me throughout this whole experience. I am really blessed to have you as my partner in this life.

To my dearest sisters and brothers.

To all those, I dedicate this work.

Noor

2021

Acknowledgements

First and foremost, praise is to Allah, the Almighty, for giving me opportunity, determination and strength to do my research.

I am heartily grateful to my supervisor, ***Assist. Prof. Dr. Abdulsameea Jasim Abdulzehra Al-Kilabi***, whose guidance, encouragement, stimulation and insightful comments from the initial to the final step in this work, enabled me to develop my understanding on the subject and complete this study.

I would also extend my thanks and appreciation to all of my teachers in the department of Metallurgical Engineering, Faculty of Materials Engineering for their support and help.

Noor

2021

Supervisor Certificate

I certify that this dissertation entitled **"Studying the Effect of Electrode Type on the Microstructure and Mechanical Properties of Shielded Metal Arc AISI 5155 Low Alloy Steel Welds**" is prepared by **(Noor Abd Ali Kadhim)** under my supervision at the Department of Metallurgical Engineering/ Faculty of Materials Engineering/University of Babylon in partial fulfillment of the requirements for the Higher Diploma Degree in Material's Engineering/Metallurgical Engineering.

Signature:

Name of Supervisor:

Assist. Prof. Dr. Abdulsameea J. Al-Kilabi

Date: / /2022

ABSTRACT

Low alloy steels have been used to a large extent in engineering industries. They have many significant applications in the manufacture of several products such as storage tanks, oil and gas pipelines and many agricultural and construction machinery parts. These products are probably to fail during service which require to be repaired by one of the welding processes. On the other hand, shielded metal arc welding is considered the most common and widespread welding processes. The study aims to investigate and compare the mechanical properties (tensile and hardness) and microstructure resulting from the use of different electrodes (E6013, E7018, E8018-B2, E316L-16 and ENiCI) with the shielded metal arc welding of 6 mm thickness AISI 5155 low alloy steel plates. The results showed that the structure of the weld metals ranged from pearlite colonies within a ferrite matrix in addition to a needle-like structure (for E6013 and E7018) to an austenitic structure (for E316L-16 and ENiCI) passing through predominantly acicular ferrite and a small amount of pearlite colonies with ferrite at the grain boundaries (for E8018-B2). The coarsest structure in the HAZ was for all welds in the CGHAZ, in which the maximum hardness across the center of shielded metal arc welds was; where the structure contained ferrite and pearlite coarser than that of the base metal. The finest structure across the welds was in the intercritical HAZ, in which the minimum hardness was; where the pearlite might be partially spherodized. The average hardness value of the weld metal, for each weld, was lower than that of the base metal (~465 HV). The highest value was (~337 HV) for the weld resulted from the use of the E7018 electrode, whereas the lowest one was (~239 HV) for the weld achieved using the E6013 welding electrode. The maximum tensile strength and thus joint efficiency were (938 MPa and 64.6% respectively) for the weld resulted from the use of the E8018-B2 electrode, while the minimum

values were (527 MPa and 36%) for the weld achieved using the ENiCI electrode. The low cost electrode (E6013) and the expensive one (ENiCI) gave relatively poor mechanical properties, whereas the optimum properties were achieved as a result of using iron powder low hydrogen covering electrodes (E7018 and E8018-B2).

List of Tables

Table of Figures

Table of Abbreviations

Abbreviation	Definition
TTT	Time Temperature Transformation
CCT	Continuous Cooling Transformation
CGHAZ	Coarse-Grained Heat Affected Zone
AWS	American Welding Society
TIG	Tungsten Inert Gas
MIG	Metal Inert Gas
SMAW	Shielded Metal Arc Welding
AC	Alternating Current
DC	Direct Current
DCRP	Direct Current Reverse Polarity
DCSP	Direct Current Straight Polarity
ASTM	American Society for Testing and Materials
AISI	American Iron and Steel Institute
HAZ	Heat Affected Zone
BM	Base Metal
WZ	Weld Zone
FGHAZ	Fine Grain Heat Affected Zone
SAW	Submerged Arc Welding

Table of Contents

CHAPTER ONE:

INTRODUCTION

CHAPTER ONE: INTRODUCTION

1.1 General Review

Alloy steels have been developed for several reasons, one of the most important of which is to get rid of the limitations of the use of carbon steels. With the use of carbon steels, a tensile strength higher than ($700N/mm^2$) cannot be obtained, if toughness and ductility are also required. Carbon steels also have poor resistance to corrosion. Alloy steels are generally stronger and have thermal and corrosion resistance higher than carbon steels, in addition to hardenability, machinability and ductility. This is due to the adding of alloying elements to steels with different weight percentages **[1,2]**. These types of steels have many applications. Rails, rocker panels, door beams, and bumpers are the most common **[3,4]**.

Shielded metal arc welding (SMAW) is one of the most popular welding processes in the world, accounting for more than half of all welding processes in some countries. Because of its versatility and simplicity, it is particularly dominant in the maintenance and repair industry, and is extensively used in the construction of steel structures and in industrial fabrication. Given the low equipment cost and wide application, the process is likely to remain popular, especially among amateurs and small businesses where specialized welding processes are uneconomical and unnecessary. The shielding characteristics of the electrodes make the process less sensitive to wind and draft than gas shielded arc welding processes.

SMAW process is often used to weld carbon steels, low and high alloy steels, stainless steels, cast iron and ductile iron **[5]**.

1.2 The Aims of the Present Work

The aim of this study is to investigate and compare the mechanical properties (tensile and hardness) and microstructure resulting from the use of different electrodes with the SMAW of low alloy steels for manufacturing of many engineering industries in the agricultural and energy fields.

1.3 The Scope of the Present Work

This dissertation consists of five chapters which can be briefly described as follows:

- Chapter one: deals with a general introduction related to this study and its objectives.

- Chapter two: begins by giving important details about the raw material used (low alloy steels); gives describes and details about the welding of low alloy steels by using shielded metal arc, the basic work principle of this process, electrodes used; highlights the advantages, disadvantages and applications of this process. This chapter also deals with a literature review.

- Chapter three: presents a description of the experimental part in terms of the use of low alloy steels as a raw material, welding electrodes in addition to the welding method. The manufacturing and preparation of the samples for mechanical and physical testing were also described.

- Chapter four: includes all the experimental results of the work that have been obtained and discussing them in details.

- Chapter five: gives the main conclusions obtained from this investigation with recommendations for the possible future works.

CHAPTER TWO:

THEORETICAL PART &

LITERATURE REVIEW

CHAPTER TWO: THEORETICAL PART AND LITRERATURE REVIEW

2.1 Introduction

This chapter deals with steels, their types, mechanical properties, hardenability and thus weldability. It also describes the factors that affect hardenability. The welding process used to join steels particularly shielded metal arc welding have also been explained. In addition, the advantages, disadvantages and applications in addition to electrodes used with this process have been clarified. A literature review for studies about the present work has also been highlighted.

2.2 Steels

As is known, Steel is an alloy of iron that contains carbon ranging by weight between 0.02% and 2.11% (most steels range between 0.05% and 1.1%C). It often includes other alloying ingredients, such as manganese, chromium, nickel, and/or molybdenum; but it is the carbon content that turns iron into steel. Hundreds of compositions of steel are available commercially **[6]**.

2.3 Types of Steels

There are a number of ways by which steel can be classified. However, the most widely popular classification is based on their chemical composition as provided by the American Iron & Steel Institute (AISI) they are **[7]**:

1. Carbon Steels
2. Alloy Steels
3. Stainless Steels
4. Tool Steels

2.4 Importance of Steels

Steel is the second largest man-made material; second only to cement. Steel has been known to the societies for centuries, and has been closely associated with the progress of civilization through the ages. Steel has established itself by far as the most important multi-functional and highly adoptable material. Its production cost is low compared to other materials, it is less energy consuming and most competitive, when its high strength to weight ratio is considered cost. Steel scraps are 100% recyclable and steel plant by-products are largely re-usable for gainful purpose like in the manufacturing of cement and fertilizers. Steel is said to be the material whose applications are not limited by choice, but by imaginative ability of our mind **[8]**.

2.5 Mechanical Properties of Steels

Each steel grade, following international standards, reflects the measured mechanical properties of the material **[9]**:

Strength refers to the force needed to deform a material. The strength of steel can be improved through some heat treatment such as normalization, which creates a uniform microstructure throughout the material.

Hardness is the material's ability to resist abrasion. Increasing the carbon content and quenching the material results in improved hardness.

Ductility refers to the ability of a metal to plastically deform under stresses. By annealing the cold-formed steel, its low ductility can be improved, as annealing enables the reforming of crystals, thus eliminating the dislocations in the microstructure.

Machinability refers to how easy it is for steel to be ground, cut or drilled. It is greatly affected by hardness. As hardness increases, machining becomes more difficult.

Toughness is the ability of a material to resist stress without fracturing. Toughness can be improved by adding spheroids in the microstructure as in tempering.

Weldability refers to the ease with which a material can be welded without defects. Heat conductivity, along with melting point and electrical conductivity can influence the weldability of a material. It is mainly dependent, however, on the heat treatment used and the chemical composition of the material.

2.6 Hardenability of Steels

Hardenability is a measure of the ease with which steel can be hardened by heat treatment and is strongly affected by alloying elements. The hardenability of steel determines the depth and distribution of hardness induced by quenching. It is the ability of the material to become uniform or to harden in the depth direction. Variation in structure in incomplete hardenability will lead to a corresponding variation in properties **[10]**.

Maximum hardness is achieved when a fully martensitic structure is formed, so steels that can be fully hardened over wide ranges of cooling rates are deemed to have good hardenability. The time temperature transformation (TTT) curve (Figure 2.1) can provide immediate evidence of a steel's hardenability **[11]**.

2.6.1 Time Temperature Transformation and Continuous Cooling Transformation Diagrams

Time Temperature Transformation (TTT) and Continuous Cooling Transformation (CCT) diagrams can be used to predict steel microstructures as a function of cooling rate from austenite temperatures. Each diagram is only applicable to a single steel composition.

TTT diagrams are developed by heating the steel into the austenite temperature range, followed by rapidly cooling to various temperatures, and then holding at each of these temperatures to allow for transformation from austenite to take place. Because they rely on isothermal transformation, they are often called Isothermal Transformation Diagrams. CCT diagrams do not involve holding the specimen at a single temperature; they are generated by allowing the steel to cool continuously from austenite at various cooling rates. As a result, CCT diagrams are more representative of real welding conditions, and therefore commonly used for predicting weld microstructures. TTT curves that are shifted more to the right (longer times) indicate greater hardenability since the formation of 100% martensite can occur at slower cooling rates as compared to a less hardenable steel. There are a number of factors that control the hardenability of a steel. Alloying additions have the greatest effect on

hardenability because they are effective in delaying the transformation to other transformation products (ferrite, pearlite, bainite) during cooling.

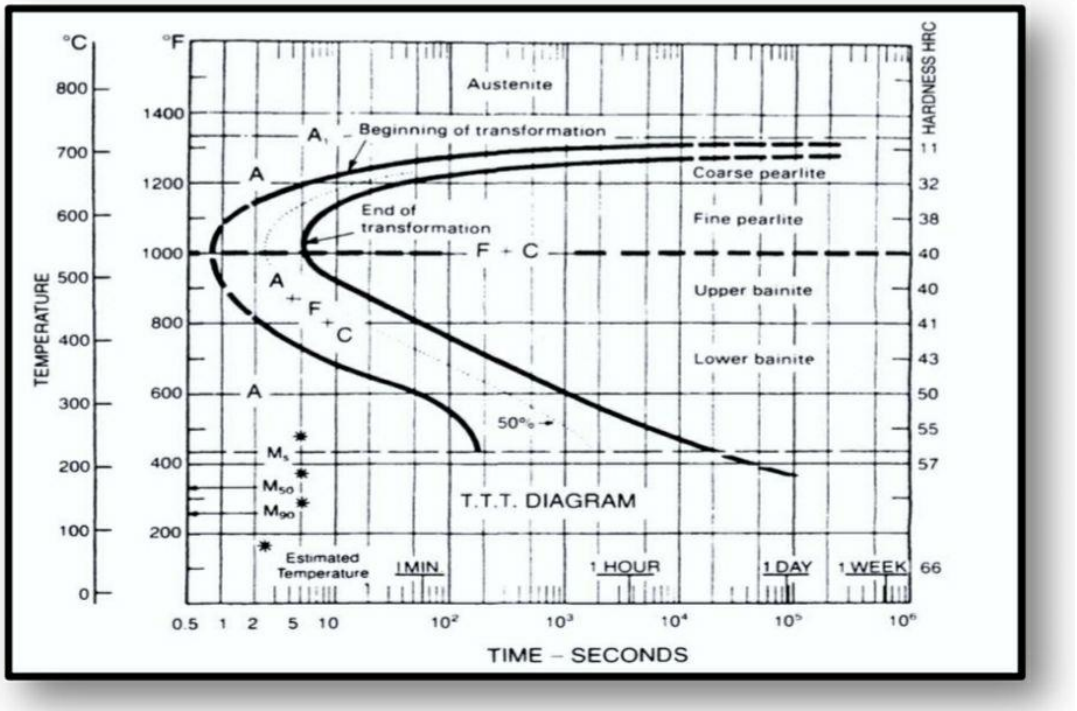

Figure 2.1: Isothermal transformation curve for a plain carbon steel **[12]**.

Large grain sizes of austenite will slow the transformation to ferrite/pearlite allowing martensite to form, thereby increasing hardenability. The coarse-grained heat affected zone (CGHAZ) of steels have large grain sizes, so martensite may more easily form in this region than what the TTT predicts. Increases in carbon content not only increase the hardness of the martensite but also play a role in increasing the hardenability as well. Finally, the thickness of the steel indirectly plays a role in hardenability since it affects cooling rates. During heat treating, thin plates or small diameter bars may be readily hardened by quenching, since heat extraction is quite rapid. Thick plates or large forgings are less hardenable during heat treating because of the variation in cooling rate from surface to center. However, when welding, thicker sections will produce faster weld cooling rates that increase the likelihood for martensite formation. This is because with thicker plates, cooling occurs in three dimensions instead of two **[11]**.

2.6.2 Factors that Affect Hardenability

The following points highlight the four main factors affecting the hardenability of steel. The factors are:

2.6.2.1 Grain Size

The effect of grain size is similar to that of alloy additions. Increasing the grain size retards the diffusion of carbon (a further distance to travel), promoting the formation of martensite. Nucleation of pearlite occurs at prior austenite grain boundaries. With a coarse grain size, there is less surface area at the grain boundaries to nucleate. Finer grain size increases the grain boundary area and promotes nucleation of pearlite. The higher nucleation rate at finer grain sizes will result in the decrease of time needed to complete the formation of pearlite. As the grain size increases, the hardenability increases **[13]**.

2.6.2.2 Transformations of Austenite

Heat treatment of steels requires that the component be heated into the austenite phase range. Once the part is thoroughly heated into the austenite range, then the part is cooled in a controlled condition to achieve the desired microstructure. With hypoeutectoid steel, if the part is cooled slowly, the microstructure will consist of pearlite and ferrite; if cooled rapidly, the part will consist of martensite. If an intermediate cooling rate is achieved, bainite or a mixed microstructure will result. The required rates to achieve the desired microstructures are governed by the carbon and alloy content. For many heat-treated products, the desired microstructure is martensite. Martensite provides a hard microstructure for high wear applications. It is also brittle and must be tempered to improve ductility. Non-martensitic transformation products such as pearlite and bainite are avoided because they reduce hardness **[13]**.

2.6.2.3 Composition (Carbon and Alloying Elements)

Increasing the carbon content tends to retard austenite transformation. This enables a slower quench for reduced distortion while maintaining hardness. The as-quenched hardness of an alloy is only dependent on the amount of carbon present. Additional alloying elements do not increase the achievable maximum as-quenched hardness of the steel. Alloying elements, such as nickel, chromium, and others, retard diffusion of carbon within the steel. This diffusion of carbon is needed for the formation of pearlite. Martensite formation is promoted. Therefore, alloying elements promote the formation of martensite and allow martensite formation at lower quenching rates. This enables a part to be more deeply hardened **[13]**.

2.7 Weldability of Steel

Weldability is the capacity of a metal or combination of metals to be welded into a suitably designed structure, and for the resulting weld joint(s) to possess the required metallurgical properties to perform satisfactorily in the intended service. Good Weldability is characterized by the ease with which the welding process is accomplished, absence of weld defects, and acceptable strength, ductility, and toughness in the welded joint. Factors that affect weldability include welding process, base metal properties, filler metal and surface conditions. The welding process is significant. Some metals or metal combinations that can be readily welded by one process are difficult to weld by others. For example, stainless steel can be readily welded by most arc welding processes, but is considered a difficult metal for oxyfuel welding **[6]**.

2.7.1 Transformations in the Weld Metal

In fusion welding, the existence of solid grains at the liquid-solid interface works as ready nuclei from which the granular growth releases **[2]**. In steel alloys, the weld metal solidifies forming a solid solution of C, Mn and some other elements with iron. Based on cooling speed, the resulting grains might be dendritic or columnar. Heat typically flows from the weld zone towards the colder metal adjacent to this zone. The weld metal therefore, has columnar grains with right angles to the fusion line. This is what distinguishes grains resulting from single-pass welding. With multi-pass welding, and due to repeated heating, these grains transform into equiaxid grains, where each welding pass reheats the previous pass. This reduces the particle size of the formed grains, consequently improving the mechanical properties of the weld zone **[1]**.

Increasing the carbon content does not increase the weld metal strength as it does, e.g., with the wrought steel, because such an increase causes segregation of carbon during the solidification. This leads to the formation of cementite during the subsequent solid-state transformation of austenite, decreasing the toughness of the weld metal. Therefore, the carbon content in the weld metal should be kept low as (0.1%) as a maximum. This ratio should therefore not be exceeded in the welding electrodes, whatever the strength desired of the weld metal, or the carbon content in the base metal. When the carbon content of the weld metal is maintained low, the microstructure will mostly be a mixture of ferrite and carbides with a very small proportion of bainite or martensite. The microstructure of the base metal however varies from ferrite to martensite, based on the ratio of carbon and alloying elements in steels **[14]**.

2.7.2 Thermal Effects of SMAW on the Base Metal and its Mechanical Properties

The base metal adjacent to the weld zone is typically divided into two zones:- the heat affected zone (HAZ), and unaffected base metal **[2]**.

2.7.2.1 Heat Affected Zone

It is the region just adjacent to the weld zone which represents the base metal that is not melted by the welding heat, except that it is heated to a temperature and for a period sufficient for the occurrence of grain growth in it. This region undergoes to a complicated thermal cycles representing by sudden heating to different temperatures, ranged between melting temperature and that of the unaffected base metal. Subsequently, the heating is followed by rapid cooling due to the nearby cold metal and the surrounding atmosphere. This heating and cooling cycle serves as a different heat treatment for each region of the HAZ. This zone therefore consists of a series of structures gradient and different in their mechanical properties.

In low alloy steels, these structures might vary from the hard martensite to the coarse pearlite. The HAZ width in arc welds doesn't exceed a few millimeters. When welding low alloy steels with a single pass by SMAW process, three different metallurgical regions can be observed **[2]**:

A. Grain Growth Region: it is exactly adjacent to the fusion boundary (weld zone). In this region, the base metal is heated to temperatures in a range between above the upper critical temperature (A_3) and melting temperature (Figure 2.2). This resulted in coarsening the structure or grain growth **[2]**. The largest grain growth region and the maximum grain size occur as the cooling rate decreases. The cooling rate depends upon the amount of heat utilized during welding, initial temperature of the base

metal, thickness of the welds in addition to the design of the weld zone. The high initial temperature of base metals and weld heat causes slow cooling rates, whereas the large weldment thicknesses result in rapid cooling rates. Generally, the cooling rate of this region is greater than those in the other regions of the HAZ, because of the severe thermal drop from the temperature of this region to that of the cold base metal **[2]**. This region is therefore the hardest of the HAZ in weldments of low carbon steels **[14]**.

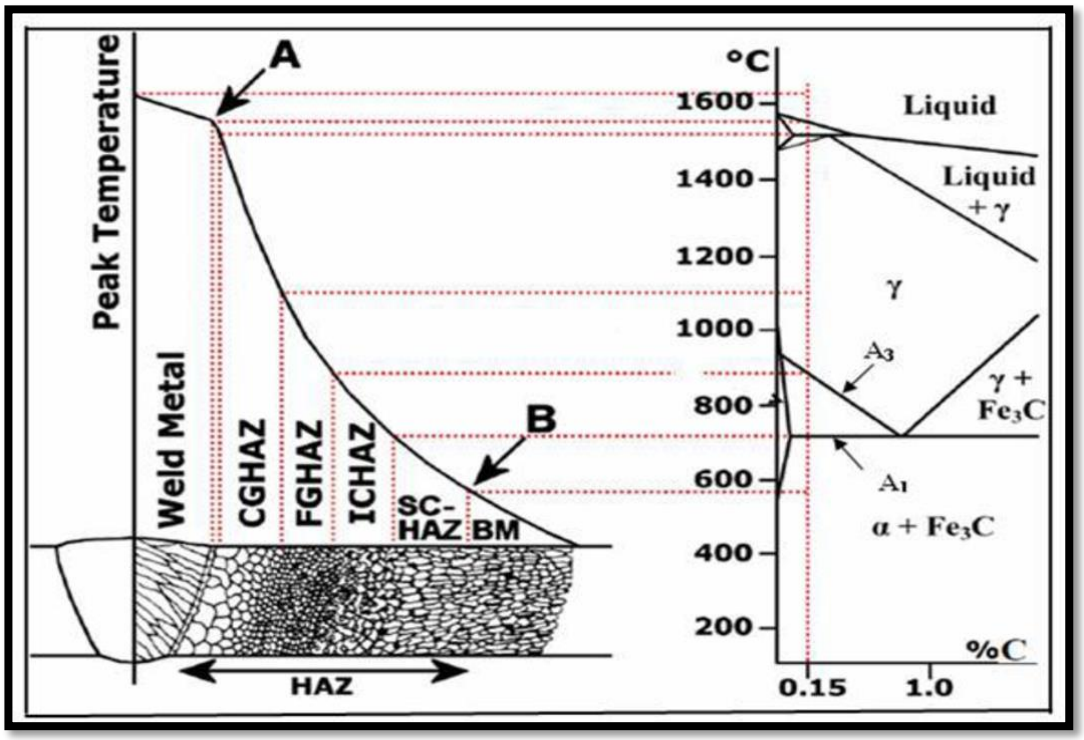

Figure 2.2: The Fe-C phase diagram **[15]**.

The microstructure in this region based on the ratio of carbon and alloying elements, grain size and the cooling rate. In weldments of low carbon steels, the structure in the grain growth region is pro-eutectoid ferrite at the grain boundaries of the prior austenite, whereas the grains themselves are usually ferrite with pearlite, or ferrite with bainite. With the increase of the cooling rate or increasing the content of carbon and alloying elements, the grains of ferrite disappeared. The austenite grains then transform into bainite upper or lower, martensite or a mixture of these microstructures.

The resulting grain size depends on the grain size of the austenite. If the austenitic grains were large, the resulting structure will be coarse **[16]**. Generally, the metal in this region losses some of its ductility particularly the impact strength. Figure (2.3) shows the structure of this zone.

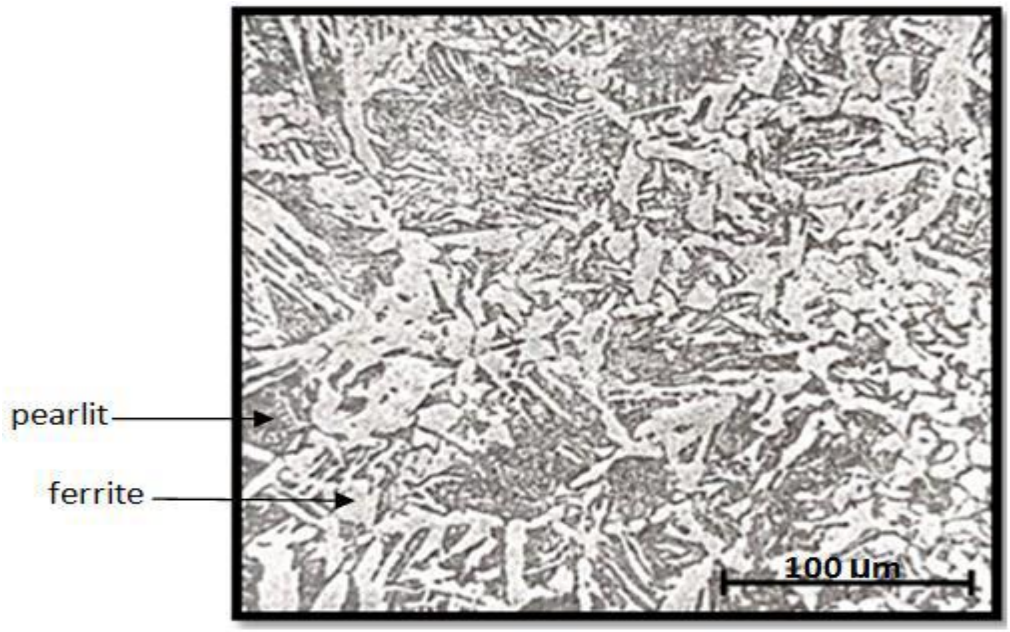

Figure 2.3: Grain growth region **[2]**.

B. Grain Refined Region: it is the region adjacent to that of grain growth, at which the metal is heated to a temperature directly above the high critical temperature (A_3) **[2]**. The metal in this zone completely transforms to a new, fine-grained austenitic structure, where the heating time isn't long enough for the growth of the austenite grains. Therefore, moderate cooling will form fine pearlitic grains. This is identical to the normalizing heat treatment implemented on carbon steels, which include heating to this temperature and then cooling with still air **[17]**. This region has relatively high strength and toughness, the same features and properties of normalized steels. Figure (2.4) shows the structure of this region, where dark areas indicate pearlite and light areas indicate ferrite.

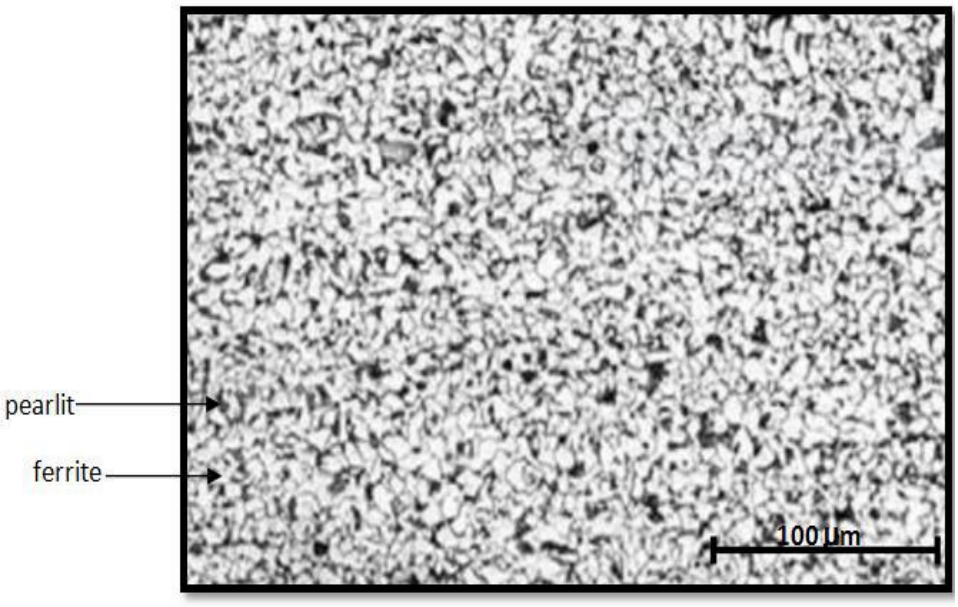

Figure 2.4: Grain refined region **[2]**.

C- Transition Region: during welding, this region is exposed to temperatures ranging between higher critical temperature (A_3) and lower (A_1) **[2]**. This heating works on transforming pearlite grains (at least partially) into fine austenite grains, but it is not sufficient to transform ferrite grains **[18]**. A partial allotropic recrystallization occurs in this region. Upon cooling, the fine austenite grains transform into fine pearlite. Obviously, in this case, the pearlite grains are reduced while the ferrite grains remain the same **[2]**. Figure (2.5) represents the microstructure of this region.

For alloy steels, this region is of particular interest, as the same cooling rate might be enough to convert the fine grains of austenite to martensite, resulting in high hardness and brittleness in this region. This exposes these kinds of steels to hydrogen cracks. Consequently, care must be followed while welding these steels to avoid such cracks. It should be noted that the main reason for the formation of martensite in this region is carbon, as with the increase in the percentage of carbon and other alloying elements, the hardenability of steels increases.

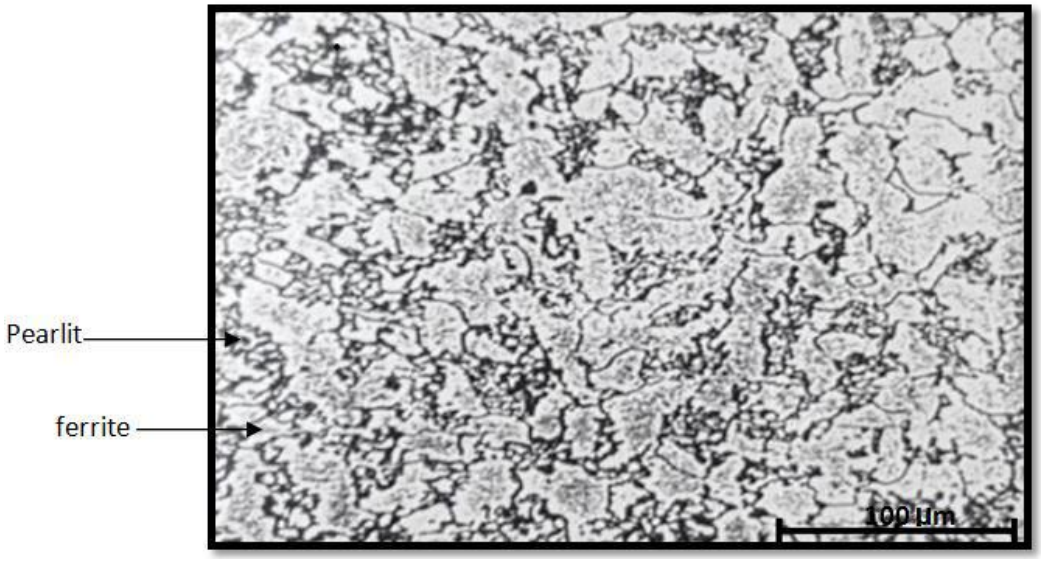

Figure 2.5: Transition region **[2]**.

2.7.2.2 Unaffected Base Metal

The base metal that is heated upon welding to temperatures insufficient to make change in its structure, comes directly after the HAZ **[2]**. Figure (2.6) shows the microstructure of the base metal of low carbon steel unaffected by welding heat.

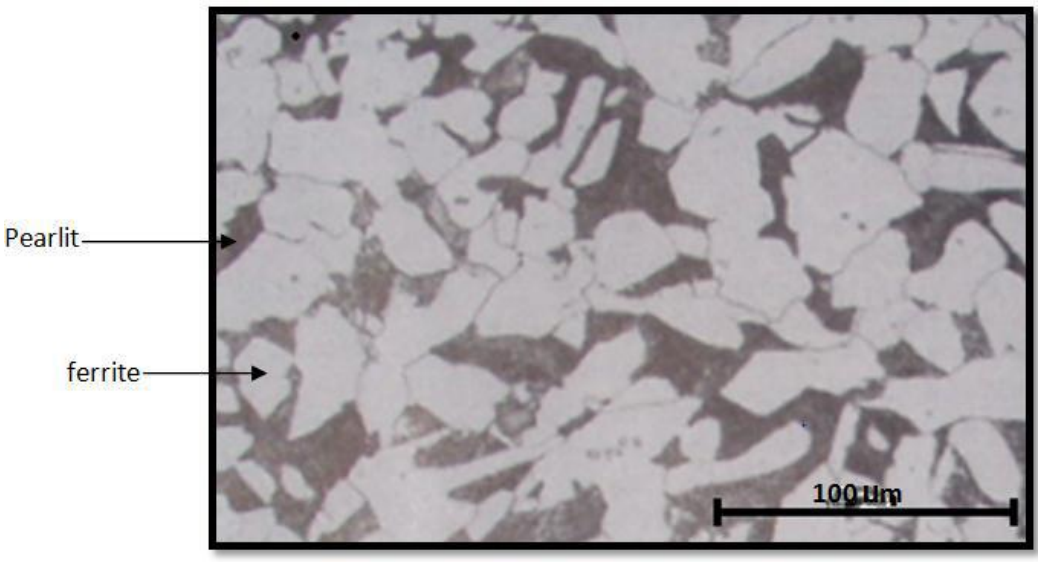

Figure 2.6: Unaffected base metal **[2]**.

2.8 The Welding of Metals

Welding is a materials joining process in which two or more parts are coalesced at their contacting surfaces by a suitable application of heat and/or pressure. In some welding processes, a filler material is added to facilitate coalescence. The assemblage of parts that are joined by welding is called a weldment **[19]**.

2.8.1 Classification of Welding Process

American Welding Society (AWS) has classified the welding processes as follows (based on the source of energy) **[19]**:

1. Gas Welding: such as Oxy-acetylene and Oxy-hydrogen welding.

2. Arc Welding: such as Carbon Arc, Shielded Metal Arc, Submerged Arc, Tungsten Inert Gas (TIG), Metal Inert Gas (MIG) and Plasma Arc welding.

3. Resistance Welding: such as Spot, Seam, Projection and Flash Butt welding.

4. Solid State Welding: such as Friction, Ultrasonic, Explosive, Forge and Diffusion welding.

5. Thermo-chemical Welding: such as Thermit welding.

6. Radiant Energy Welding: such as Electron Beam and Laser Beam welding.

2.9 Shielded Metal Arc Welding

Shielded metal arc welding (SMAW) is a process that uses a consumable electrode consisting of a filler metal rod coated with chemicals that provide flux and shielding. The SMAW (sometimes called stick welding) electrode is typically 225-450 mm long and 2.5-9.5 mm in diameter. The coating consists of powdered cellulose (i.e. cotton and wood powders) mixed with oxides, carbonates and other ingredients held together by a silicate binder. Metal powders are also sometimes included in the coating to increase the amount of filler metal and to add alloying elements. The heat of the welding process melts the coating to provide a protective atmosphere and slag for the welding operation. It also helps to stabilize the arc and regulate the rate at which the electrode melts. During operation the uncoated metal end of the welding stick (opposite the welding tip) is clamped in an electrode holder that is connected to the power source. The holder has an insulated handle so that it can be held and manipulated by a human welder. Currents typically used in SMAW range between 30 and 300 A at voltages from 15 to 45 V. Selection of the proper power parameters depends on the metals being welded, electrode type and length, and depth of weld penetration required **[20]**.

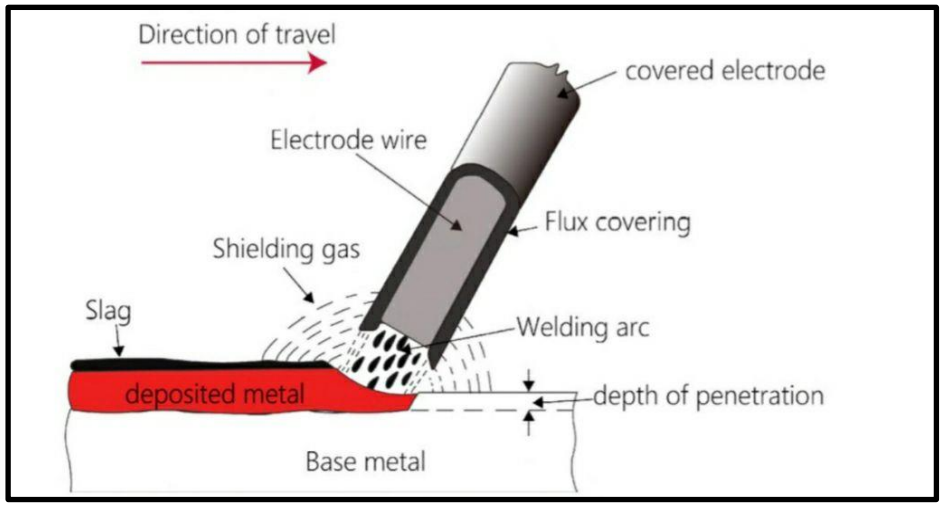

Figure 2.7: Schematic representation of shielded metal arc welding **[21]**.

2.9.1 Principle of Operation

The principle of SMAW is a consumable electrode method in which base metal and welding rod melt and unite using the heat of arc which occurs between cladding welding rod and base metal, and is usually called as arc welding. According to this welding method, welding rod and base metal melt by the heat of arc (Figure 2.7), and transfer to molten weld pool, making weld metal. At this time, the depth into which base metal melts is called penetration. Welding rod is one whose circumference of metal core wire is painted by covering material, and covering material is decomposed by arc heat, and thus stabilizes arc. Occurred gas or slag then prevent molten metal from contacting oxygen or nitrogen at atmosphere, and thus prevents the oxidation and nitrification of molten metal. In addition, good weld metal can obtained by adding required alloying element to core wire and covering material, and it is refined as molten metal by adequate chemical reaction. If a weld by uncoated rod, there is no protection, and thus one cannot prevent oxidation and nitrification, one cannot obtain good weld metal, and because arc is also not stabilized, it is difficult to use important subsidiary materials by non-cladding welding rod **[21]**.

2.9.2 Flux Functions

Flux has several benefits and the most important of which are **[22]**:

1. Provides shielding gas that isolates air from the weld zone and adjacent zones.

2. Most fluxes contain deoxidizers and nitrogen absorbers.

3. Provides a layer of slag on the weld metal which protects the molten or hot weld zone from air, in addition to protect the weld zone from rapid cooling after welding.

4. Contains materials that are easily ionized when heated by arc, such as sodium and potassium. These materials help to stabilize the electric arc and to maintain the gap connected between the tip of electrode and the work piece.

5. Flux is sometimes used to add alloying element to the weld metal. It sometimes contains the iron powder that increases deposition rates.

2.9.3 Electric Power for Welding

The equipment used in arc welding provides an electric current, which may be either alternating current (AC) or direct current (DC). The amount of current (amperage) is adjustable based on the diameter of the electrode and thickness of the base metal.

With a DC arc welding circuit, two terms are used to define electrical flow:

1- DCRP: Reverse polarity-Electrode positive.
2- DCSP: Straight polarity-Electrode negative.

Reverse Polarity (DCRP): The arc welding cables are arranged so that the electrode is the positive pole and the base metal is the negative pole in the arc circuit **[23]**, as shown in Figure (2.8).

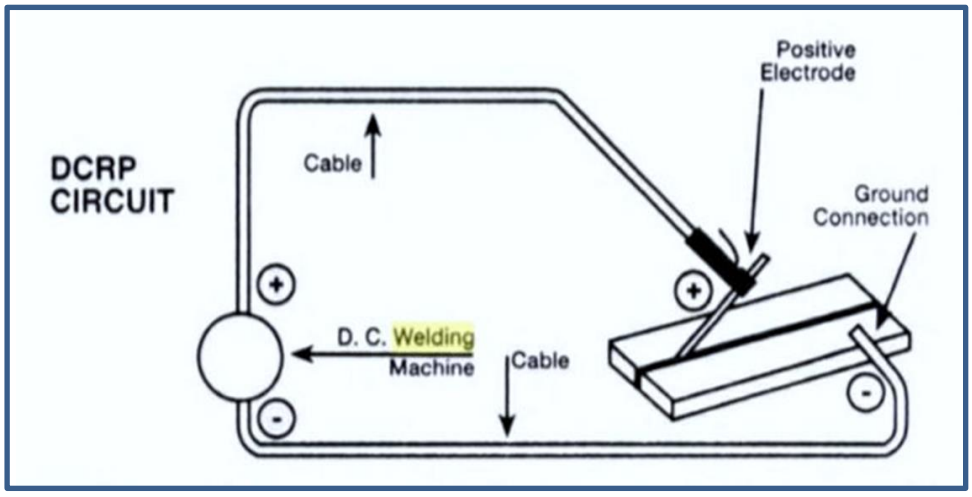

Figure 2.8: Reverse polarity **[23]**.

Straight polarity (DCSP): The arc welding cables are arranged so that the electrode in the negative pole and the base metal is the positive pole as shown in Figure (2.9). In general, the DCSP will provide shallow penetration in comparison to the DCRP **[23]**.

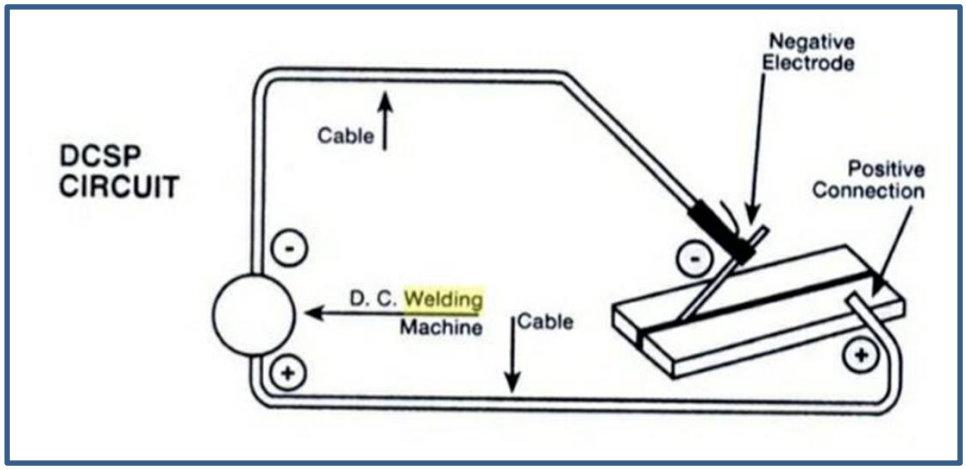

Figure 2.9: Straight polarity **[23]**.

2.9.4 Welding Electrodes

In arc welding, the welding rod is called the filler metal or electrode which is the main material that fills up the gap between the base metals. For the arc welding rod, there are an uncoated electrode and a covered electrode. The uncoated electrode is mainly used for automatic or semi-automatic welding, and the covered electrode is used for manual arc welding. Various types of shielded arc electrodes are made according to the materials of the metal welded. The shielded arc welding electrode is usually dried, and one tip is not covered in order that 25mm of the tip can be connected to current holding between holders **[20]**.

The choice of electrode for SMAW depends on a number of factors, including the weld material, welding position and the desired weld properties **[5]**.

2.9.5 Classification of Electrodes

Metal arc electrodes may be grouped and classified as uncoated electrodes, thinly coated electrodes and heavy coated electrodes. A classification number series (formulated by the American Welding Society-AWS) has been adopted by the welding industry to identify electrodes by means of this numbering system **[24]**. Figure (2.10) shows how to set the type of electrodes made of low carbon steels and low alloy steels according to AWS system **[16]**.

Below examples of electrodes used with the SMAW process **[25]**.

The **E6013** electrode is designed to be used with AC or DC, either polarity, rutile electrode and it is relatively insensitive to rust or other surface impurities. It deposits smooth weld beads in all positions and the slag is easy to remove. It is very easy to strike and restrike, making it ideal for short welds, root runs and tacking.

The **E7018** electrode is designed to be used with DC, a reliable, general purpose electrode specially made for mild and low-alloy steels. It deposits a tough, crack-resistant weld metal. It is insensitive to the composition of the base material within rather wide limits.

The **E8018-B2** electrode is also designed to be used with DC. It is suitable for welding creep resistant steels of the 1.25Cr0.5Mo type. The electrode welds with a quiet, stable arc and produces a minimum of spatter loss. It deposits a weld metal which is resistant to cracking as well porosity.

The **E316L-16** electrode is designed to be used with AC or DC, It is a rutile electrode with extra low carbon content for welding stainless steel type 316L, 18Cr12Ni3Mo. The electrode is especially designed for position welding of thin walled pipes. It is very easy to strike and restrike.

The **ENiCI** electrode is also designed to be used with AC or DC, A nickel-cored electrode for welding normal grades of cast iron. The weld metal is soft and easily machinable. The electrode is suitable for joining cast iron for the rectification of casting and the repair of broken parts.

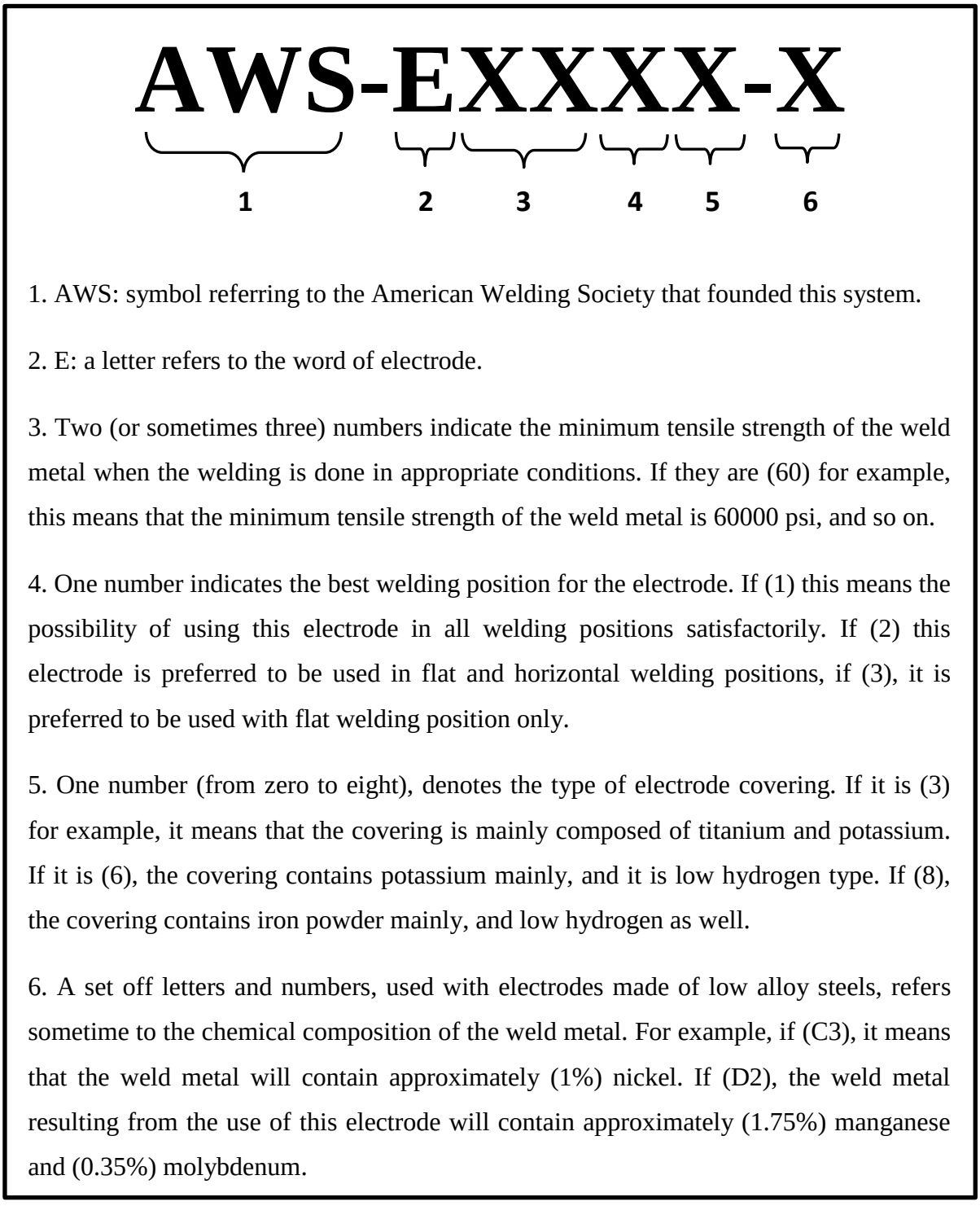

Figure 2.10: The designation system used by the American welding society for electrodes made of low carbon steels and low alloy steels **[16]**.

2.9.6 Advantages of Shielded Metal Arc Welding Process

The main advantage of SMAW is the large variety of metals and alloys with which the process can weld. Procedures and electrodes are available to weld carbon and low alloy steels, high alloy steels, tool and die steels, stainless and heat resisting steels, cast irons, copper and copper alloys, plus nickel and cobalt alloys **[26]**.

Following are other advantages of the process **[26]**:

1. The equipment is relatively simple, inexpensive and portable.
2. The electrodes provide both the shielding and the filler metal to make a sound weld.
3. Auxiliary gas shielding or granular flux is not required.
4. The process is less sensitive to wind and draft than the gas shielded arc welding processes.
5. The dimensions of the electrodes are ideal for reaching into areas of limited access (electrodes can be bent, and with the aid of mirrors, applied in blind spots).
6. The process is suitable for most of the commonly used metals and alloys.
7. The process is flexible and can be applied to a variety of joint configurations and welding positions.
8. Optimum results can be readily and reliably obtained.

2.9.7 Drawbacks of Shielded Metal Arc Welding Process

The main drawbacks of SMAW are **[27]**:

1. Not recommended for welding metals less than 1.6 mm thick.
2. Excessive spatter.
3. Slag cleanup is required.
4. Produces weld beads with rough surfaces.

5. Welds are subject to porosity.
6. Arc blow must be controlled.
7. Frequent stops and starts are required to replace electrodes, resulting in a lower electrode deposition rate than the gas metal arc welding.
8. Greater possibility of weld defects as a result of frequent stops and starts.
9. Some electrode waste (about 10 percent from discarded stub loss).
10. Potential electric shock from open-circuit voltage.
11. The SMAW process produces large amounts of fumes and smoke.

2.9.8 Applications of Shielded Metal Arc Welding

The SMAW process has widespread use on farms and ranches, in auto repair facilities and home and equipment workshops, and in other areas where maintenance and repair work is required. It is still a widely used process in pipelining and structural steel construction. SMAW can be used to weld carbon steel, low alloy steel, high strength steel, cast iron, malleable iron, bronze, nickel, stainless steels and aluminum in all thicknesses. The SMAW process is also used for hard surfacing **[28]**.

2.10 Literature Review

The literature survey covers the researches concerned in one way or another with the present work.

Syahroni et al. (2006) [29] investigated the effects of the proper electrode selection on mechanical properties of underwater wet welded-Joints. Three different types of electrodes for SMAW namely E6013, E6019, and E7018 were selected to perform underwater wet welding of the mild steel ASTM A36 plate. Tension and bending tests were carried out according to ASTM and AWS D1.1 standards respectively. The yield and tensile strengths of the welded joints fulfilled the acceptance criteria. The weld joints using E6013 and E6019 electrodes have satisfied the minimum criteria of

elongation, but two specimens of the welded joint using E7018 electrode have failed. Welded joints using E6013 and E6019 have also satisfied the acceptance criteria of bending test, but have failed when using E7018 electrode. The failure of the welded joint using E7018 electrode to meet the elongation and bend test might be caused by the presence of a large amount of fine pearlite phase in HAZ which made the welded joint less ductile.

Verma et al. implemented in **(2016) [30]** a comparative study on the effect of electrode type on the microstructure and mechanical properties of dissimilar welds of 2205 austeno-ferritic and 316L austenitic stainless steels. The welds were achieved by SMAW using two different electrodes namely duplex (E2209) and austenitic (E309L). The microstructure across the welds was evaluated by using optical microscopy and scanning electron microscopy (SEM), while, the localized chemical information was obtained by energy dispersive spectrometer (EDS). In the E2209 weld metal, the solidification was observed as the primary ferrite mode, while the 309L weld metal was observed as the primary ferrite with austenitic matrix. Optimum ferrite content was observed in both electrodes. Finally, it was concluded that for the joints between the 2205 austeno-ferritic and 316L austenitic stainless steel, the E2209 electrode was dominant property wise.

In (2018), Tahir et al. [31] studied the mechanical properties of AISI 1020 low carbon steel welds under different types of welding fillers (E6013, E7016 and E7018) and currents (80A and 90A) for SMAW. This study utilized the Design of Experiment (DOE) by adopting the Full Factorial Design, and the experiment was analyzed using the two way ANOVA. The results proved that there are significant effects of welding filler types and current levels on the tensile strength and hardness of the welded metal. At the same time, the ANOVA results and interaction plot indicated that there are significant interactions between the welding filler types and the welding

current on both the hardness and tensile strength of the welded metals, which has never been reported before. This study found that when the amount of heat input increases, the mechanical properties such as tensile strength and hardness decrease. The optimum tensile strength for the welded metals was produced by the E7016 filler, and the optimum hardness was produced by the E7018 welding filler at welding current of 80A.

Winarto et al. (2018) [32] investigated the effect of different rutile electrodes on mechanical properties of underwater wet welded high strength low alloy AH-36 marine steel plates. Rutile electrodes used were E6013 and E7024 for SMAW with the variation of 5 m and 10 m underwater depth, and also varied with the electric current of 120A, 140A and 150A. Results showed that the hardness values increased in the areas of the weld metal and HAZ. HAZ also tended to have the highest hardness values compared to both of the weld metal and base metal. Radiography test showed that there is an incomplete penetration with all variations of welding parameters, but there is no porosity defect detected. Results also showed that the hardness value of both rutile electrodes is apbasely similar to that of the existing commercial electrode (E7014 of Broco UW-CS- 1). Moreover, the tensile test showed that the use of E6013 electrode gives better tensile properties than other rutile electrodes.

Nassar et al. (2018) [33] experimentally studied the effect of welding electrode types (E6013 and E7018) on the tensile properties of 10 mm thick AISI1010 commercial low carbon steel plates welded using the SMAW process. The results showed that the selection of different welding electrodes had a remarkable effect on the mechanical properties of the welded specimens. The increment in the electrical current for each electrode led to a decrease in the yield and tensile strengths. This behavior was attributed to the increased heat input in the HAZ.

Sumardiyanto et at. (2019) [34] studied the mechanical properties of shielded metal arc API 5L low carbon steel welds using different electrodes (E6013, E7016 and E7018). The results showed that there were significant effects of welding variables (type of electrodes and current given) on the tensile strength, impact strength and hardness of the weld metal. The results showed that for all types of electrodes when the amount of current given increases, then the mechanical properties such as tensile strength, impact and hardness decrease. The optimum tensile strength for the weld metal was produced by the welding electrode E7016 at 90A with 617.155 MPa, while the lowest value was 505.215 MPa for E6013 at 100A. The optimum hardness was produced by E7018 at welding current of 90A with 194.40 VH while the lowest was 170.60 VH for E6013 at 100A. Moreover, impact 1.915 J/mm2 by E7018 at 90A while the lowest 0.728 J/mm2 for E6013 at 100A.

Pratomo et al. studied in **(2020) [35]** the effect of welding current on the tensile strength of shielded metal arc low carbon steel welds by the use of a 3.2 mm dia. E7018 electrode. The variations of the current used were 80 A, 100 A and 130 A, and the thickness of the plate used as a base metal was 8 mm. Results found that using the current of 100 A produced the highest tensile strength value of all test specimens given good penetration results.

In **(2021), Manesh and Nasresfahani [36]** evaluated the mechanical and microstructural properties of P460NH welded micro-alloy steel utilized in pressure vessel tanks using the E8018-G electrode. The results showed that the weld zone had the highest percentage of perlite (62%), whereas the base metal had the highest percentage of ferrite (73%). In addition, the HAZ had the highest hardness value (298 HV) while the base metal had the lowest (210 HV).

Yousaf et al. (2021) [37] studied the effect of different filler materials on the mechanical properties of AISI 316L austenitic stainless steel weld Joints. SMAW for 10 mm thickness plates were performed using the E308, E309 and E316L electrodes. Results showed that the E308 filler material demonstrated better tensile properties than E309 and E316L. The hardness values are however higher for E316L filler material than for E308 and the lowest for the E309 electrode.

CHAPTER THREE:

EXPERIMENTAL PART

CHAPTER THREE: EXPERIMENTAL PART

3.1. Introduction

This chapter includes general description of the experimental work steps and describes all the conditions under which the tests were carried out. It includes materials, equipment and experimental procedures used in this study, in addition to preparing samples for the tests (cutting, milling, grinding…). Mechanical properties of the shielded metal arc welds were studied by micro-hardness and tensile tests. The changes in micro-structure of the welds were evaluated by the optical microscope. The fractography was also performed after the samples of the tensile test were fractured.

3.2 Program of the Present Study

Figure (3.1) shows the flowchart used in the present work.

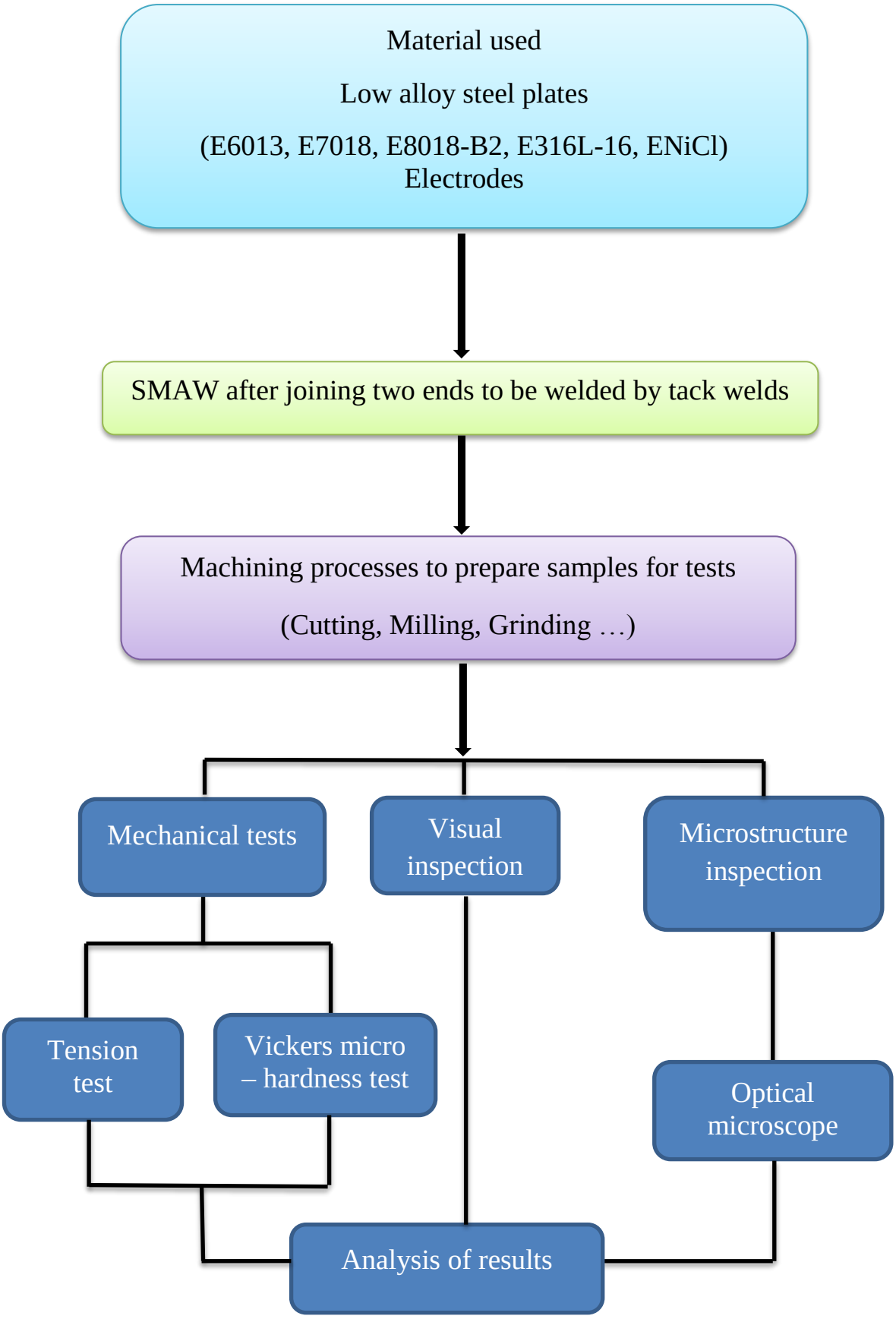

Figure (3.1): Flowchart of the present work.

3.3 Materials and their Specifications

3.3.1 The alloy used in this work: low alloy steel plates according to the specifications of American Iron and Steel Institute (AISI) **[38]**, as shown in Table (3.1), knowing that the raw material is annealed and cold drawn **[39]**.

Table (3.1): Specifications of the alloy used in the study and its chemical composition.

Alloy	**Chemical composition (wt. %)**					**Spec. symbol (AISI)**	**Shape and raw material cross section (mm)**	**Ultimate tensile strength (MPa)**	**Vickers hardness (HV)**
Low alloy steel	C	Mn	Si	Cr	P, S max.	5155	Plate (7*70)	≧1230	220
	0.51-0.59	0.7-0.9	0.15-0.3	0.7-0.9	0.04				

- The pieces to be welded were cut from the raw material, and the dimensions for each piece were (7*70*100 mm).

- Chemical composition analysis for low alloy steel was carried out using Spectromax instrument in the State Company for Inspection and Engineering Rehabilitation (SIER) shown in Figure (3.2). Table (3.2) shows the chemical composition (as an average of three readings) of the raw material used as a base metal. This composition falls within the range of the chemical composition shown in the Table (3.1).

Figure (3.2): Chemical composition analyzer.

Table (3.2): Chemical composition of the base metal.

Base metal	Chemical composition (wt. %)					
	C	**Mn**	**Si**	**Cr**	**P**	**S**
Low alloy steel	0.558	0.666	0.237	0.752	0.0105	0.0079

3.3.2 Electrodes used in this work: Table (3.3) shows specifications of the electrodes used as a filler metal with the shielded metal arc welding (SMAW) process according to the American Welding Society (AWS) **[25]**.

Table (3.3): Electrodes specifications according to AWS **[25]**.

Electrode Ø 3.2 mm	Coating type	Wire metal type	Typical properties all weld metal			Typical all weld metal composition (wt. %)						
			T.S. (MPa)	**Y.S. (MPa)**	**El. (%)**	**C**	**Mn**	**Si**	**Fe**	**Mo**	**Cr**	**Ni**
E6013	Titania-Potassium	Mild steel	510	400	28	0.08	0.4	0.3	B*			
E7018	Iron powder-low hydrogen	Mild steel	540	445	29	0.06	1.1	0.5	B*			
E8018-B2	Iron powder-low hydrogen	Low alloy steel 1.25Cr 0.5Mo	620	530	20	0.06	0.7	0.3	B*	0.5	1.3	
E316L-16	-	S.S.18 Cr12Ni 3Mo	580	480	35	0.03	0.8	0.7	B*	2.8	18.5	12.0
ENiCI	-	Ni> 90%	300	100	12	1.0	0.8	0.6	4.0			94.0

*B=balanced

3.4 Welding of Low Alloy Steels

The following procedures have been carefully performed before the start of the welding; Figure (3.3) shows the dimensions of the plate to be welded and the design of the weld joint which is a square butt joint and the welding was on both sides according to AWS.

- Removing rust from the piece surfaces using a large surface grinding machine (Russian-made, 3722 model) by (0.5 mm) from each surface, then cleaning the pieces from oils, grease and the residues of chips and other impurities.

- Drying the welding electrodes through gradual heating by furnaces from room temperature to the appropriate drying temperature of the electrodes using a vacuum drying box furnace (DZF-6020) according to the recommendations of AWS.

- Fitting-up the distance between the two pieces being welded on (2.5mm).

- Joining the two pieces to be welded at both ends by small weld beads (tack welds) with the same electrode used for welding, then removing the resulting slag.

- Adjusting the value of the welding current according to the type and size of the electrode used and the welding position. It should be within the range recommended by the manufacturer of these electrodes and according to AWS.

- SMAW of the tack welded pieces from both sides by E6013, E7018, E8018-B2, E316L-16 and ENi-Cl electrodes. Table (3.4) shows some welding conditions of low alloy steel.

- SMAW on one side of the weld joint and removal of slag produced before welding on the other side. Removing the slag due to each pass was done by a hand wire brush and welding chipping hammer.

- The welding processes were carried out on a large steel table.

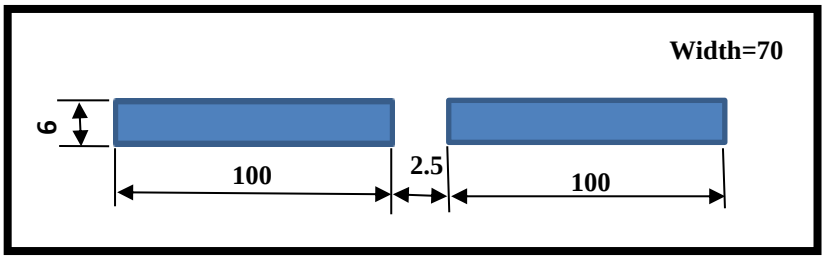

Figure (3.3): Dimensions (mm) of the plates to be joined.

Table (3.4): Welding conditions of low alloy steel.

Welding by the / Welding conditions	E6013 electrode	E7018 electrode	E8018-B2 electrode	E3016-L electrode	ENi-Cl electrode
Electrode size (mm)	3.2				
Current type	DCRP				
Position	Flat				
Current value (A)	125	140	130	130	145

3.5 Preparations of Test Samples

After welding the low alloy steels mentioned in the previous section, samples were machined from the resulting weldments for tensile, micro-hardness and microstructure tests. The following are the most important steps for the preparation of test samples.

- Straightening the weld zone (weld line), roughly, with the weldment surfaces, by a fixed head grinding machine, to facilitate weldments installing on the surface grinding machine.

- Grinding the weldment surfaces by the surface grinding machine so that the weldment can be easily clamped during subsequent stages of machining processes.

- Machining the weldment width by a universal milling machine before adjusting it by the surface grinding machine.

- Marking the dimensions of the required samples on one of the two grinded surfaces.

- Cutting the weldments according to the marking using the universal milling machine with a saw cutter with (3 mm) thickness.

3.6 Optical Microscopy

Specimens for microstructural analysis were prepared with the standard metallographic techniques. Specimens should be cut to an appropriate size for easier handling to reveal the microstructure variations in different zones. These specimens were flattened using SiC grinding papers having different roughness (180, 220, 320, 400, 600, 800, 1000, 1200, 1500 grit size). Water was used during grinding operation as a coolant in order to avoid temperature rising as a result of friction between the specimen and the grinding papers. The specimens were polished using diamond paste to produce flat, scratch free, mirror like surface. Polishing was achieved using 6, 1 and 0.25μm pastes sequentially; Grinding and polishing operations were done using polishing machine model (MP-2B grinder polisher). The specimens were etched by Nital (2% HNO_3+98%

ethanol) for (15 seconds) at room temperature, then the specimens were washed with alcohol, and dried by electric dryer. An optical microscope was then used to define the microstructure and topography of different regions on the prepared specimen surfaces across the centerline of the welds (weld zone, HAZ and the base metal). It was also used to observe and determine the type, size and location of the surface defects across the welds. This inspection was done at the Laboratory of the Metallurgical Department-Faculty of Materials Engineering-University of Babylon.

3.7 Mechanical Tests

- **Micro-hardness Test**

Micro-hardness test was carried out using digital Vickers micro-hardness tester type (HVS-1000) according to ASTM E92–17. Measurements were done across the weld centerline on both sides of the welds (weld zone, HAZ and unaffected base metal) after grinding and polishing processes of the surfaces to be measured. This test was done with load of 500 g and loading time of 10 seconds. The measurement point distribution was by 1.0 mm intervals across the welds, with three measurements per point. This test was done at the labs of the Metallurgical Department-Faculty of Materials Engineering-University of Babylon.

- **Tensile Test**

Figure (3.4) shows the shape and dimensions of the tensile test specimen used. The specimens manufactured by milling and grinding processes were as shown in Figure (3.5). Centerline of the weld was in the mid specimen and the tensile strength value was an average of two. All test specimens were notched in the weld zone with a radius of 2.5 mm to ensure that the fracture occurs in this zone. The test was carried out via universal

type device WAW-200 China (Figure 3.6) according to (ATSM E8/E8M−13a) with a speed of 1 mm/min. at the labs of the Metallurgical department-Faculty of materials engineering-University of Babylon.

G=50, W=12.5, T=6, L=200, A=64, B=64, C=20, R=13 (mm).

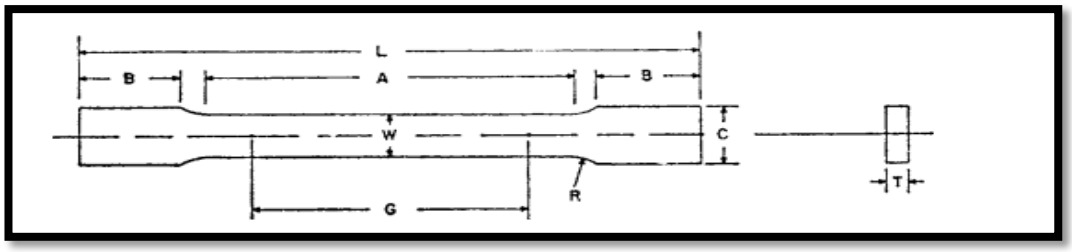

Figure (3-4): Tensile test specimen.

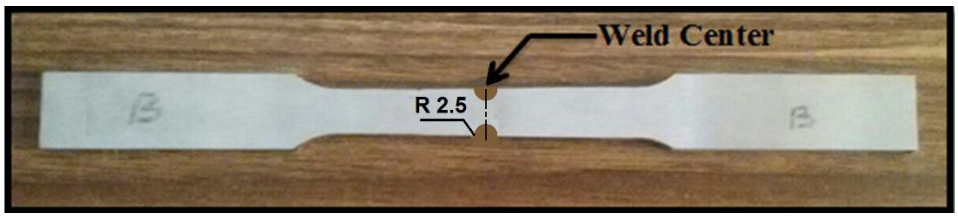

Figure (3.5): Shape of the manufactured tensile test specimens.

Figure (3.6): Tensile test device.

CHAPTER FOUR:

RESULTS & DISCUSSION

CHAPTER FOUR: RESULTS and DISCUSSION

4.1 Introduction

In this chapter, the experimental results were showed and discussed. Microstructures and microanalysis of shielded metal arc low alloy steel welds by using different electrodes have been investigated by the use of the optical microscope. Results of mechanical tests on these welds such as vickers micro-hardness and tensile strengths were also explored.

4.2 Microscopy Test

For all shielded metal arc low alloy steel welds, the microscopic examination showed variations in the microscopic structures of the weld metals depending on the type of electrodes used. It also showed variations in the heat affected zone (HAZ) starting from the region adjacent to the weld zone (grain growth region) to that which was not affected by the welding heat, passing through the grain refined and transition regions. These variations are due to the large thermal gradient to which the HAZ is exposed from the melting temperature to that of the base metal unaffected by heat. This is followed by a rapid cooling rate caused by the relatively cold adjacent base metal and the atmosphere. This heating and cooling cycle is different heat treatments for each region of the HAZ. As it is known, the difference in the nature of microscopic structures reflects a variation in properties and a difference in performance **[**2**].**

4.2.1 Shielded Metal Arc Weld using the E6013 Electrode

The microstructural examination of the low alloy steel weld joined by the SMAW process using the E6013 electrode revealed three regions: weld zone (WZ), heat affected zone (HAZ) and unaffected base metal (BM).

4.2.1.1 Weld Zone

Figure (4.1) shows that the microstructure of the weld zone exhibits pearlite colonies within a ferrite matrix in addition to a needle-like microstructure which might be a martensitic structure. During the microstructural examination of this weld, no cracking was observed in the weld zone.

As expected, the microstructure of the weld metal resulting from the use of the E6013 welding electrode, mainly consists of ferrite and pearlite, since the electrode wire type is mild steel (Table 3.3). It is known that the weight percentage of the electrode metal within the deposited weld metal is the main. However, pearlite appeared in a greater proportion than expected, due to the effect of dilution with the base metal, a low alloy steel.

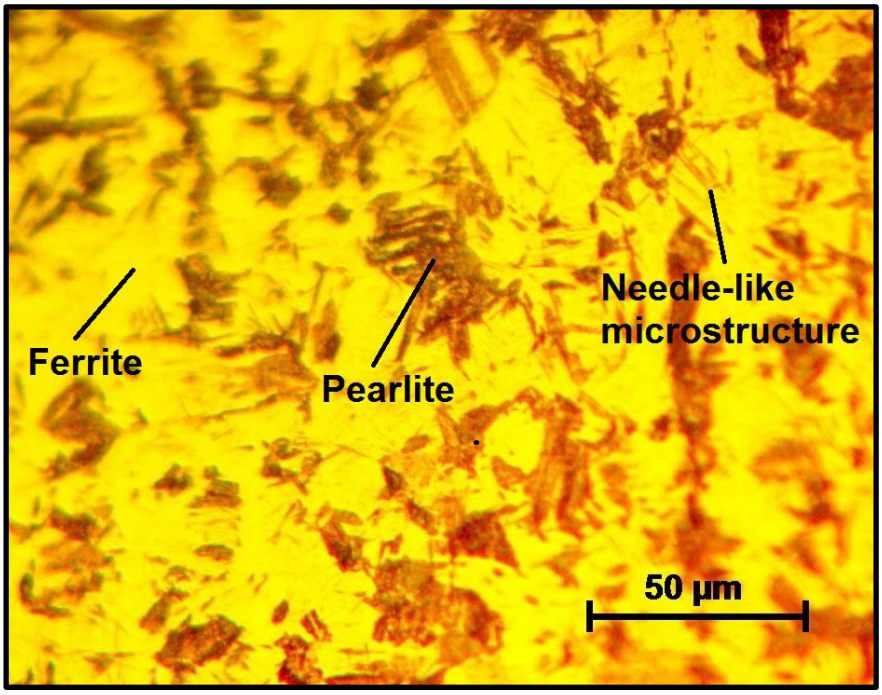

Figure (4.1): The microstructure of the shielded metal arc weld zone.

4.2.1.2 Heat Affected Zone

The microstructure of the HAZ is divided into three regions as follows:

Coarse Grain Heat Affected Zone (CGHAZ): it is the region directly adjacent to the weld zone which is subjected to a higher temperature compared to other regions of the HAZ, so, this region has coarse grains. The microstructure of this region is mostly coarse ferrite and pearlite and even coarser than those of the base metal, in addition to a small amount of a needle-like microstructure (Figure 4.2a). The resulting particle size depends on the grain size of the austenite. Generally, the cooling rate of this region is greater than those in the other regions of the HAZ, because of the severe thermal drop from the temperature of this region to that of the cold base metal **[2,18].** This region is therefore the hardest of the HAZ in low carbon steel welds **[40]**. Moving away from the weld center of the joint, the grain size of the coarse grained zone gradually decreases up to the FGHAZ.

Fine Grain Heat Affected Zone (FGHAZ): it is the region adjacent to the grain growth region within which the region just above A3 in the Fe-Fe$_3$C phase diagram is subjected to a temperature so that the grain growth is slight and the grains remain fine. The microstructure of this region shows a a grain size of ferrite and pearlite smaller than that of the base metal (Figure 4.2b). However, there is no evidence on boundaries separating the CGHAZ and FGHAZ.

The heat treatment to which the grain refined region is subjected is identical to the *normalizing* heat treatment which is typically applied on carbon steels. The properties of this region is therefore comparable to those of the normalized steel.

Transition Region (Intercritical HAZ): Figure (4.2c) shows the microstructure of this region; the region adjacent to the FGHAZ (between A1 and A3). The finest grain size across the weld can be observed in this region, where the pearlite might be partially spheroidized. This is in agreement with that obtained by Albhate (2021) **[41]**.

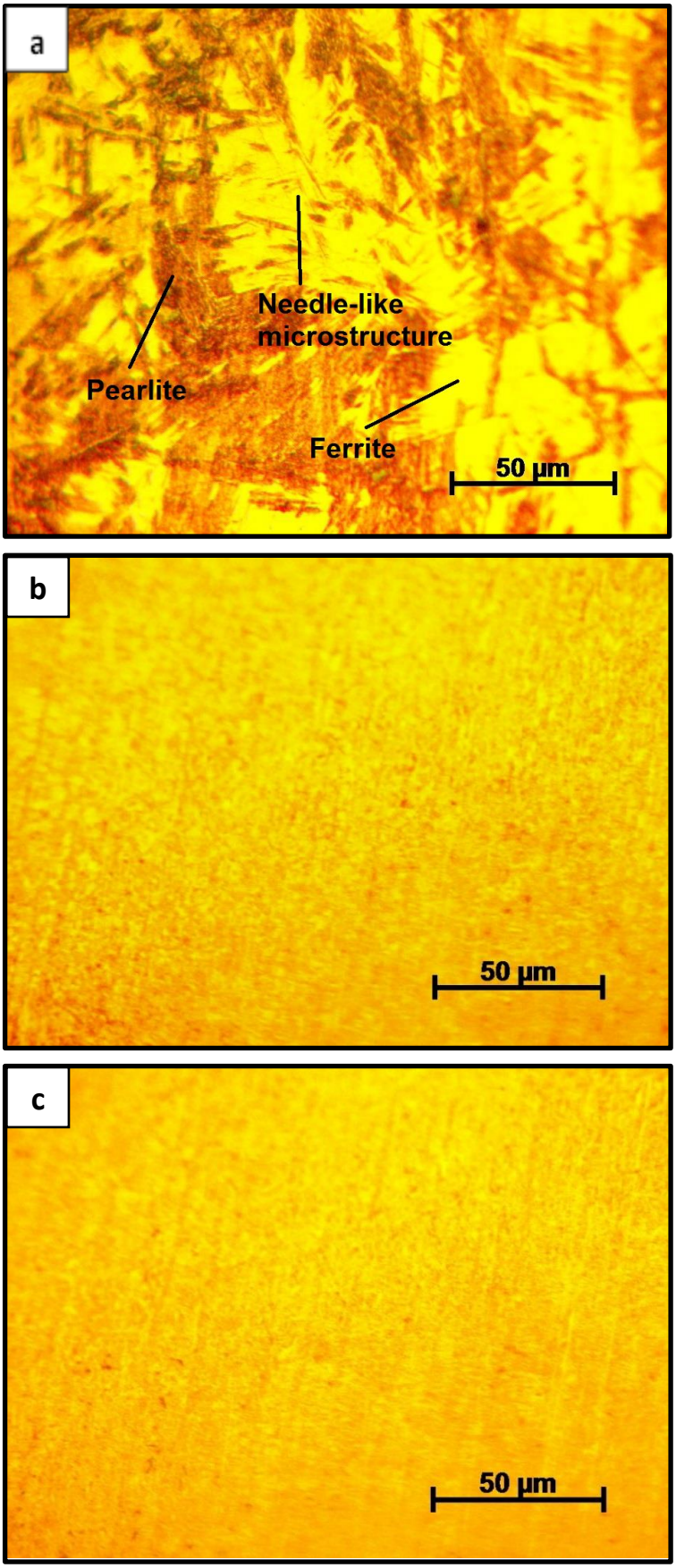

Figure (4.2): Microstructure of the (a) grain growth region, (b) grain refined region and (c) transition region of the shielded metal arc weld using the E6013 electrode.

4.2.1.3 Unaffected Base Metal

This part of the base metal comes immediately after the HAZ, where the microstructure exhibits a very small amount of pro-eutectoid ferrite at the grain boundries in addition to pearlite and ferrite grains (Figure 4.3) depending on the chemical composition of the base metal (Table 3.2).

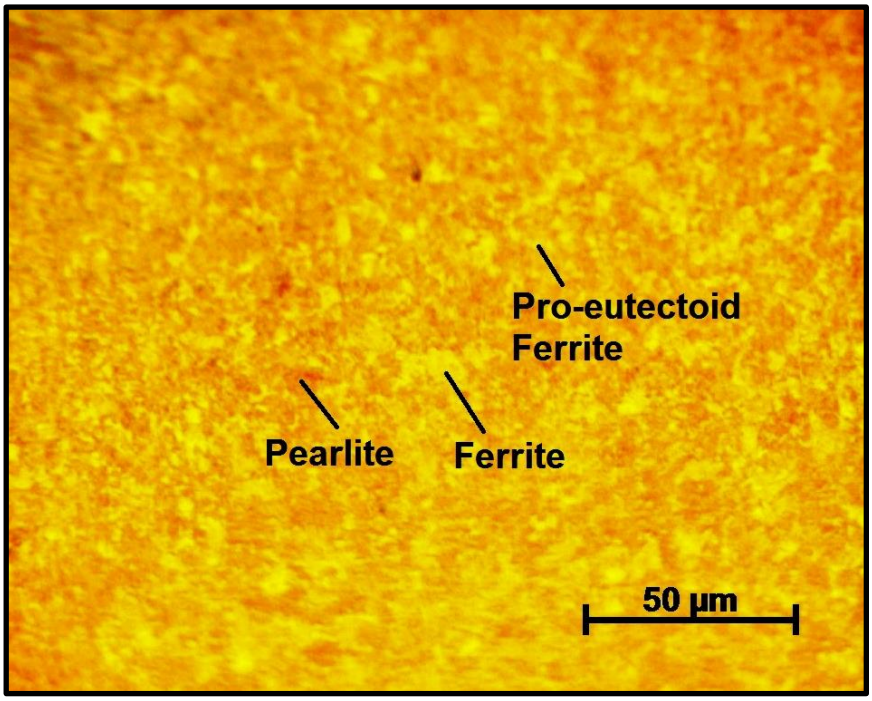

Figure (4.3): The microstructure of the low alloy steel base metal.

4.2.2 Shielded Metal Arc Welds using Different Electrodes

The microscopy test of low alloy steel welds joined by the shielded metal arc welding (SMAW) process using different electrodes (E7018, E8018-B2, E316L-16 and ENiCI) revealed variuos structures of the weld metals (Figure 4.4). The HAZ structures of these welds were similar to those exhibited in the weld achieved using the E6013 electrode.

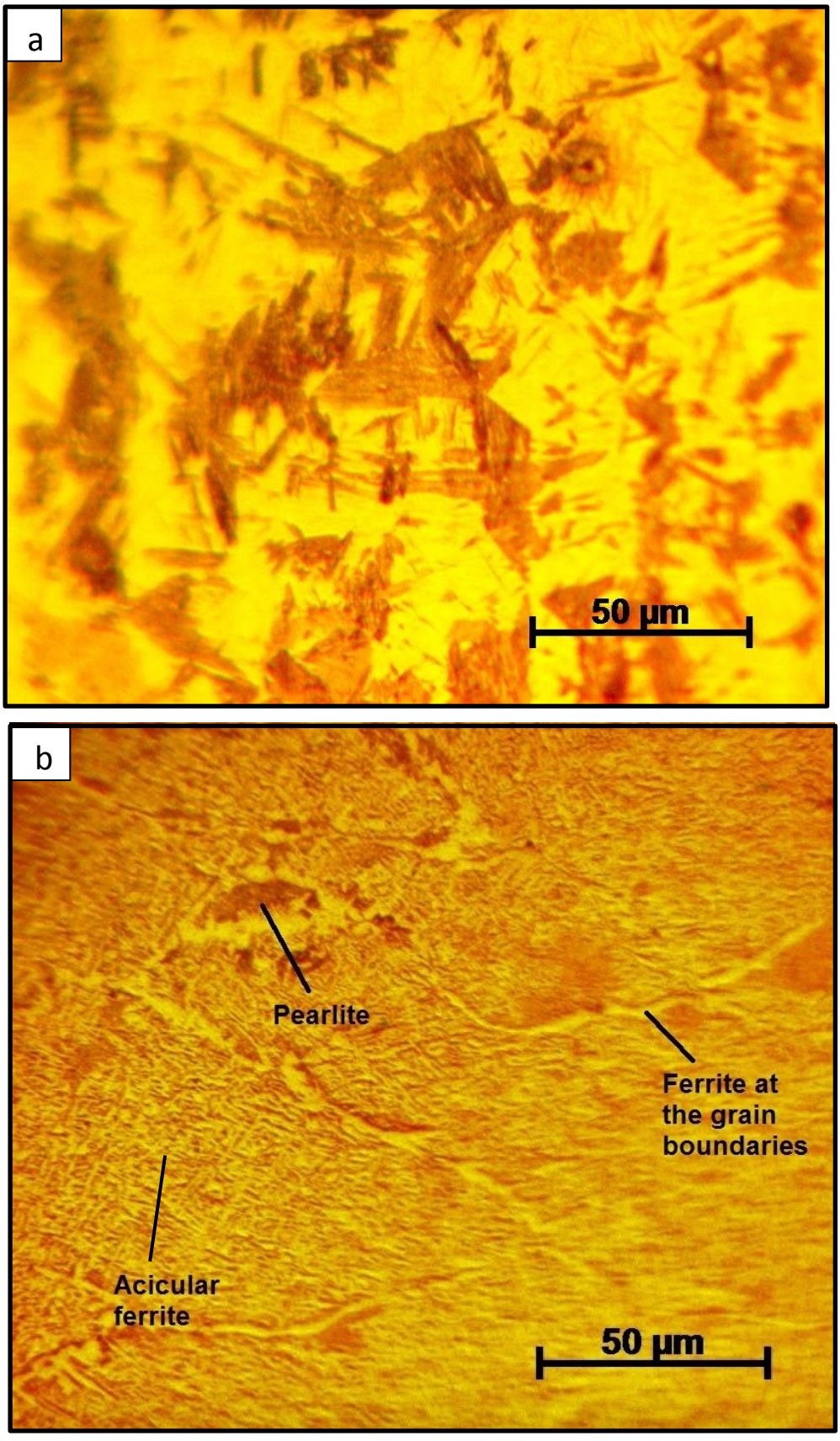
a
50 µm
b
Pearlite
Ferrite at the grain boundaries
Acicular ferrite
50 µm

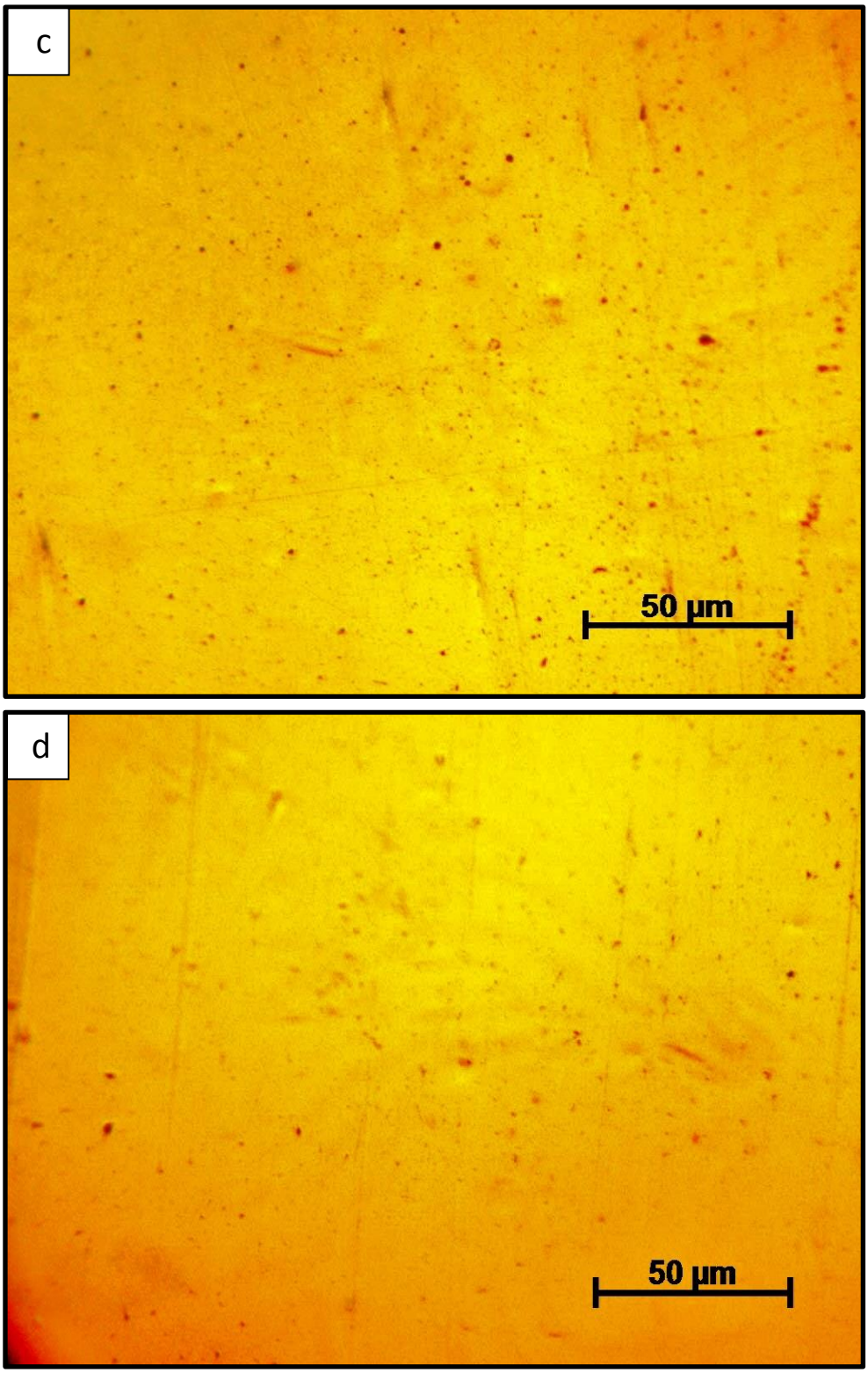

Figure (4.4): The microstructure of the shielded metal arc welds by using (a): E7018, (b): E8018-B2, (c): E316L-16 and (d): ENiCI electrodes.

It is clearly observed from the Figure (4.4 a) that the microstructure of the shielded metal arc low alloy steel weld using E7018 electrode was similar to that of the E6013 one. This is because that the weld metal microstructure resulting from using the E7018 electrode, mainly consists of ferrite and pearlite, since the electrode wire type is mild steel too (Table 3.3). Figure (4.4 b) exhibits that the microstructure of the weld resulted from using the E8018-B2 electrode was predominantly acicular ferrite and a small amount of pearlite colonies with ferrite at the grain boundaries. This is in agreement with that obtained by **Trindade et al. (2007) [42]** which might be due to the presence of 1.3% Cr and 0.5% Mo in the typical all weld metal composition (Table 3.3). Due to the fact that E316L-16 and ENiCI welding electrodes have relativelly high percentages of nickel (Table 3.3), the microstructures of the weld metals resulted from using these types of electrodes generally seem to be only gamma phase (Figure 4.4 c and d). Figure (4.5) shows the interface between the WZ and CGHAZ of the weld resulted from the use of the ENiCI electrode.

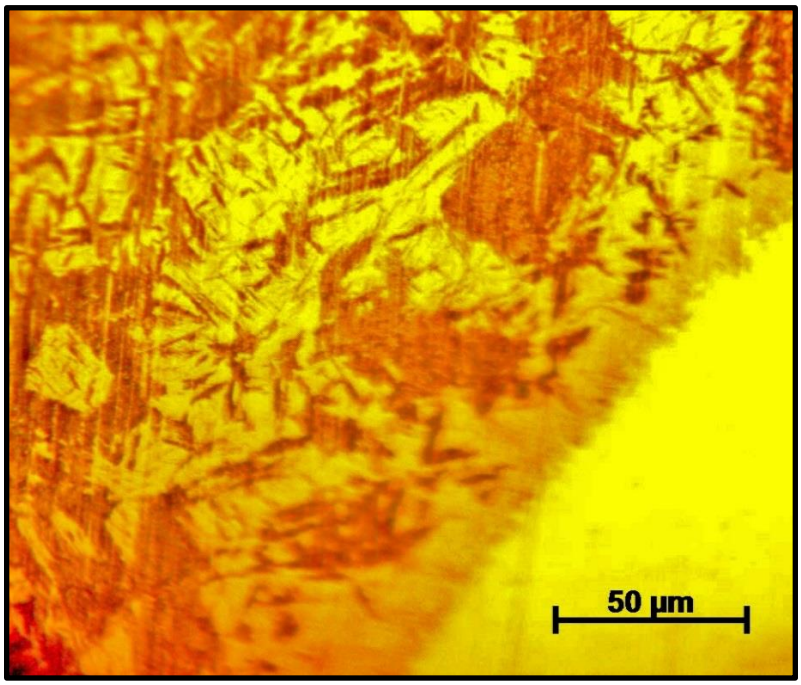

Figure (4.5): Interface between the austenitic microstructure WZ and CGHAZ of the weld achieved using the ENiCI electrode.

4.3 Micro-hardness Test

Since there was a series of microstructural changes across the welds, it was expected that the hardness varies too.

The hardness test is the easiest way to estimate the quality of the weld, and thus the weld performance; it is also important as a way of distinguishing the weld zones.

4.3.1 Shielded Metal Arc Weld using the E6013 Electrode

Figure (4.6) shows the hardness distribution across the low alloy steel weld (on cross section) joined by SMAW process using the E6013 electrode. Hardness varies on advancing from the weld center (point 1) towards the unaffected base metal (point 4). The hardness value sharply rises on moving from the weld center (~239 HV) towards the unaffected base metal up to the maximum value across the weld (~741 HV) at a 5 mm distance away from the weld center (point 2). Moving towards the unaffected base metal, the hardness decreases to the minimum value across the weld (~353 HV) at a 12 mm distance away from the weld center (point 3). The hardness then increases to the base metal hardness value (~465 HV) at about 20 mm distance away from the weld center (point 4).

The average hardness in the weld centre (point 1) is lower than that of the base metal (point 4). The reason behind this is the high proportion of the soft ferrite phase in the weld center (Figure 4.6-1) compared to that in the base metal (Figures 4.6-4), because the weld metal consists of the molten filler metal and the molten base metal. The filler metal was generally made of low carbon steels (Table 3.3).

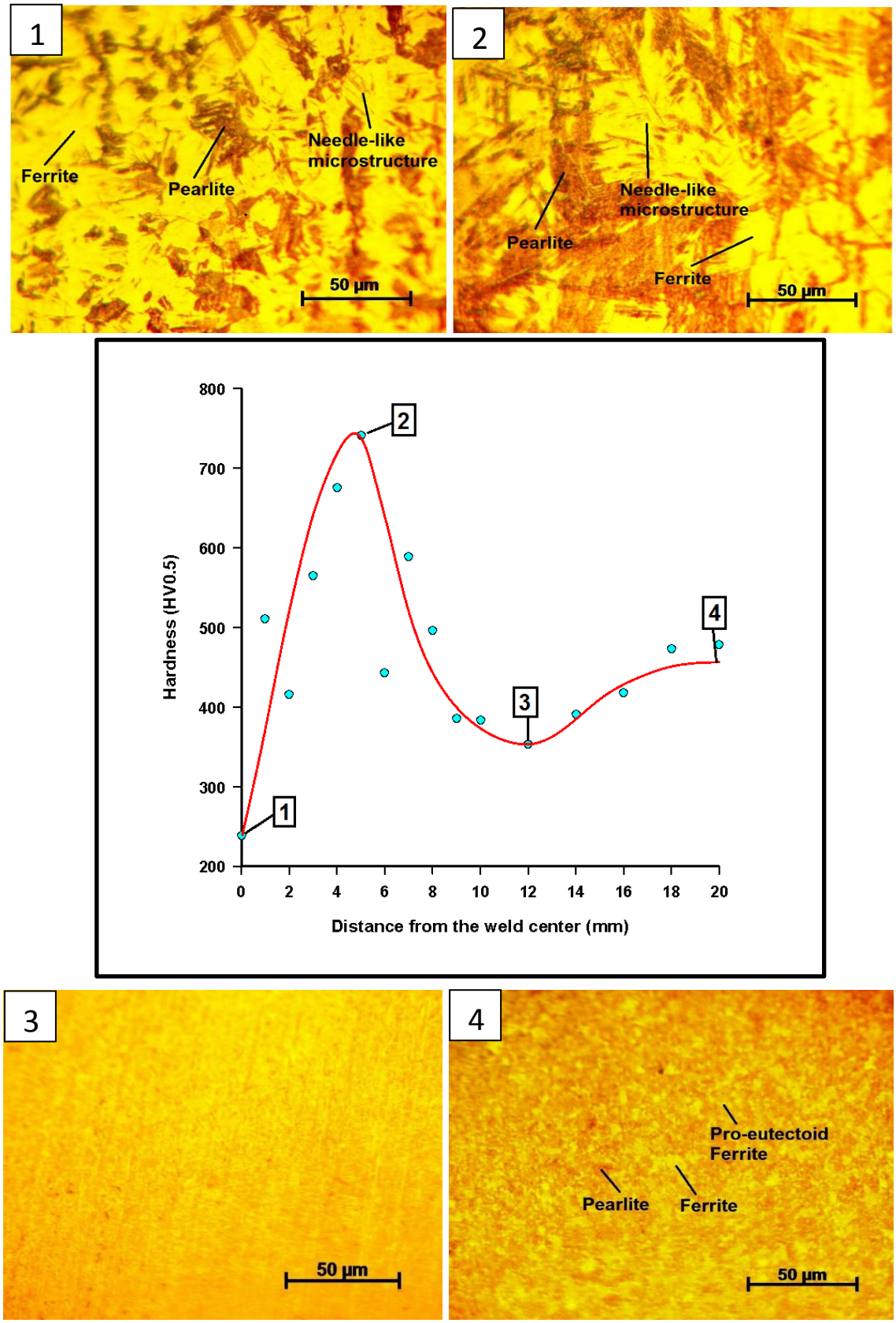

Figure (4.6): The hardness distribution across the low alloy steel weld joined by SMAW process using the E6013 electrode, (1): weld center (2): CGHAZ (3): intercritical HAZ (4): unaffected base metal.

The maximum hardness across the weld was at a region of a small distance away from the weld centre (point 2). A possible reason for this rise in hardness is the decrease of the soft ferrite phase in the microstructure of this region. The cooling rate in this region is generally higher than in the other regions of the HAZ due to the severe thermal gradient from the temperature of this region to the temperature of the cold base metal. Since quicker cooling rates lead to smaller interlamellar spacings in pearlite **[43],** the hardness is thus higher. This rapid cooling rate might be the reason behind the needle-like microstructure pesented in this region which may be another cause for this value of hardness. The minimum hardness across the weld (point 3), observed in the intercritical zone (Figures 4.6-3), could be attributed to the partially spheroidized pearlite structure in this zone which consists of a partially spheroidised cementite in a soft ferrite matrix.

4.3.2 Shielded Metal Arc Welds using Different Electrodes

Figure (4.7) shows the average hardness values of the welds using the different electrodes (E6013, E7018, E8018-B2, E316L-16 and ENiCI). It is clearly observed that the average hardness value increased significantly while using the E7018 electrode; it is the highest value among the welds. The reason for this relatively high value might be the weight percentage of manganese (1.1%) in the weld metal resulting from the use of this electrode (Table 3.3). The average hardness value resulting from the use of the E8018-B2 electrode has decreased compared to that of E7018 due to the presense of acicular ferrite at the expense of the perlite (Figure 4.4b). Figure (4.7) also shows that the hardness values have decreased in the welds caused by using the (E316L-16 and ENiCI) electrodes respectively. The reason for these values is the austenitic structure of these welds (Figure 4.4c-d) due to the high weight percentages of nickel in the typical all weld metal composition (Table 3.3).

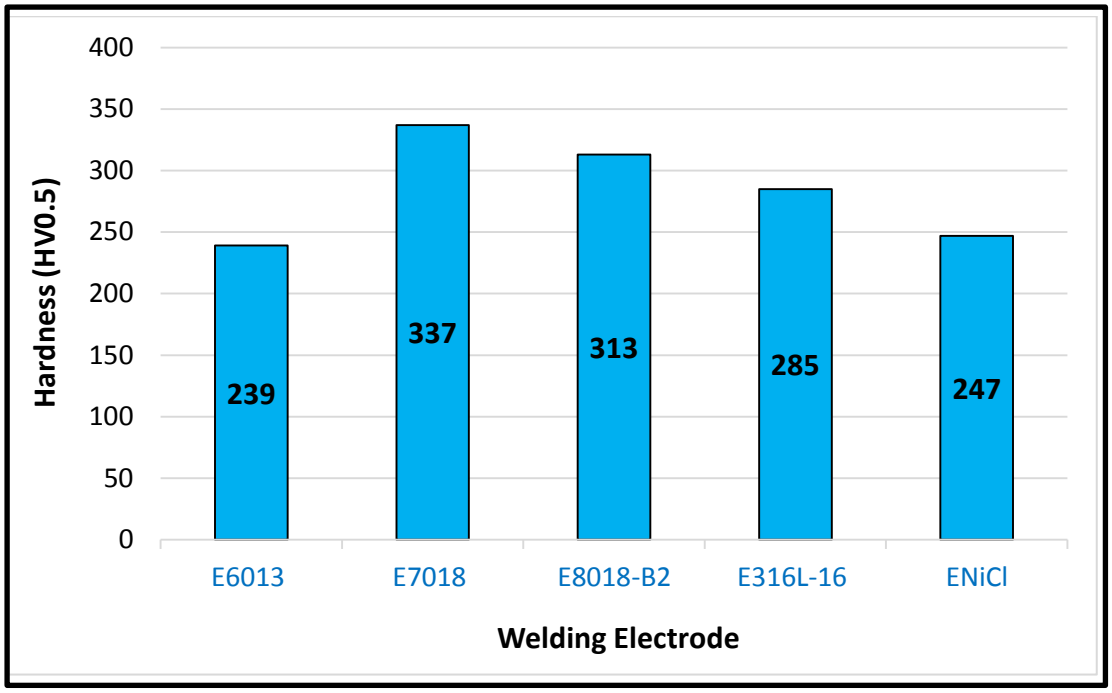

Figure (4.7): The average micro-hardness values in the center of the shielded metal arc welds using the different electrodes.

4.4 Tensile Test

The tensile test specimens were manufactured so that the weld center is in the mid of the specimen. All specimens were fractured from the weld zone. Figure (4.8) shows the average tensile strength of tensile test specimens prepared from the shielded metal arc welds, and Figure (4.9) presents the load-displacement curve for one of the arc weld tensile specimens.

The steel type (AISI 5155) was selected as a base metal for being one of the most difficult low alloy steels to weld due to its high hardenability as a result of its relatively high contents of carbon and alloying elements **[2,44].**

Since all tensile test specimens were fractured from the weld zone, the results shown in the Figure (4.8) represent the average tensile strength values of the weld metals.

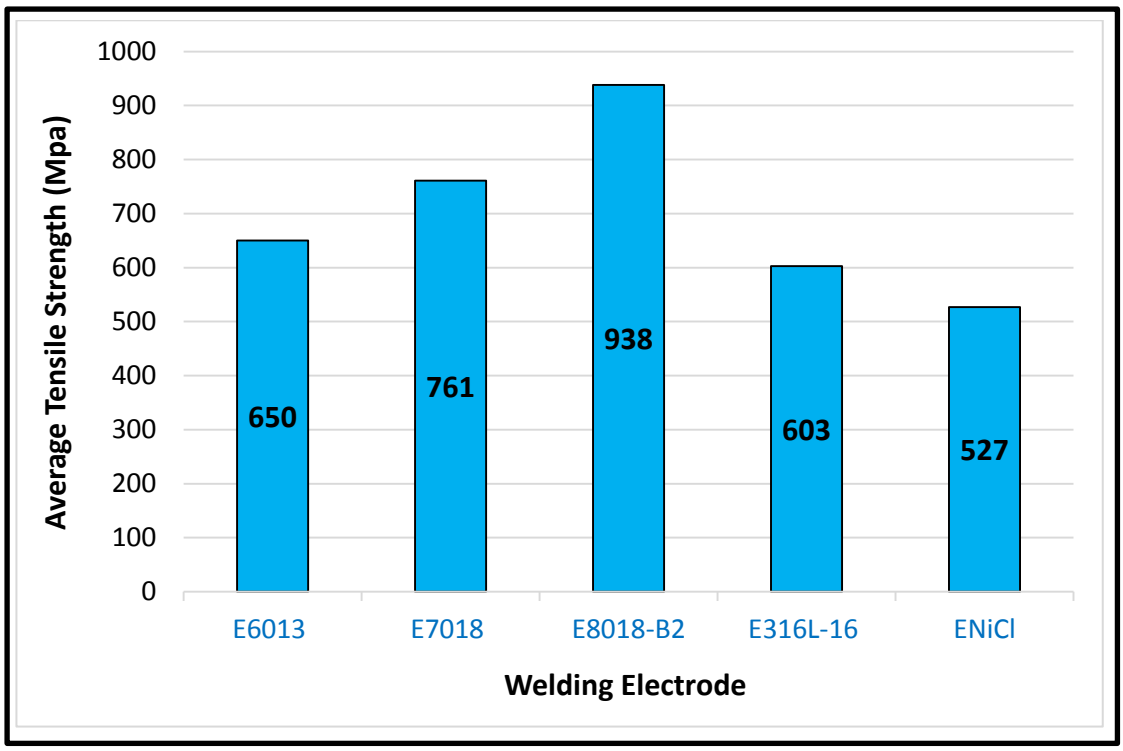

Figure (4.8): Tensile strength of the shielded metal arc welds.

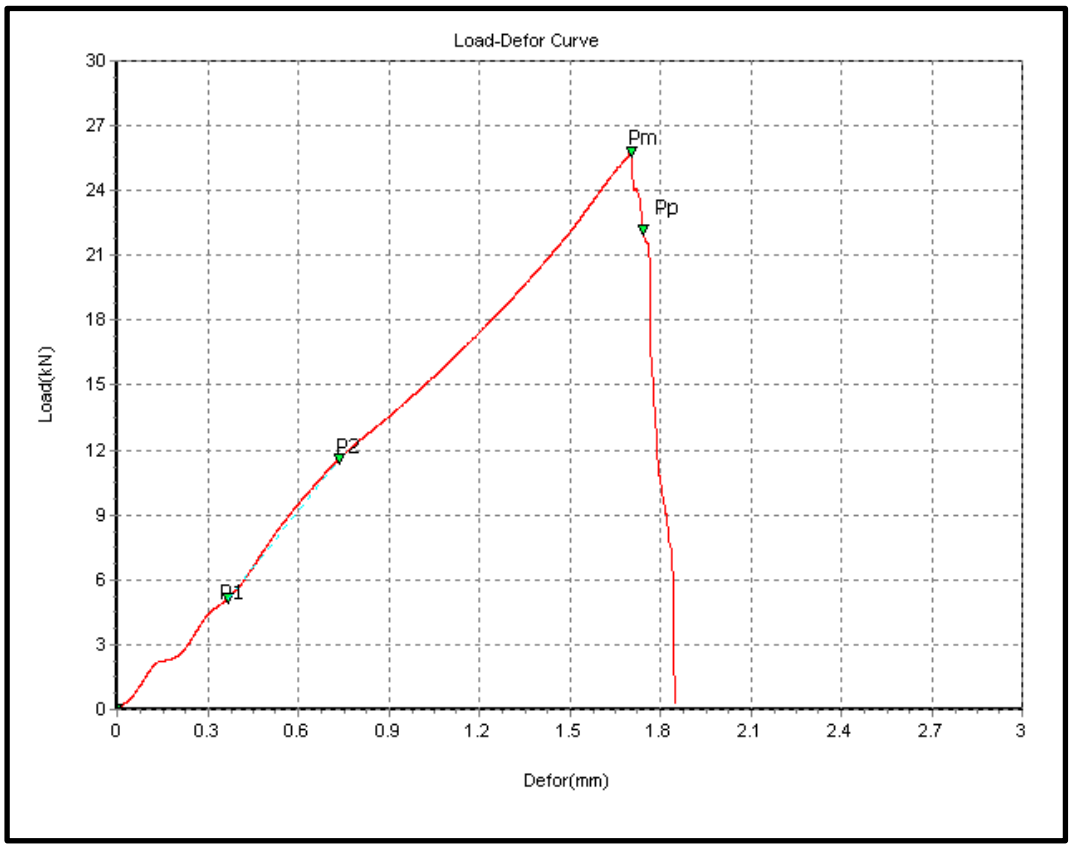

Figure (4.9): The load- displacement curve for one of the arc weld tensile specimens (using the ENiCI welding electrode).

Mean while, the average tensile strength of the base metal specimens was (1452 MPa). Thus, the weld joint efficiency for each weld could be calculated by using the following relationship **[2]**.

$$\textbf{Weld joint efficiency (\%)} = \frac{\textbf{Weld metal tensile strength}}{\textbf{Base metal tensile strength}} * \mathbf{100} \qquad \textbf{(4.1)}$$

Figure (4.10) shows the joint efficiency for each weld.

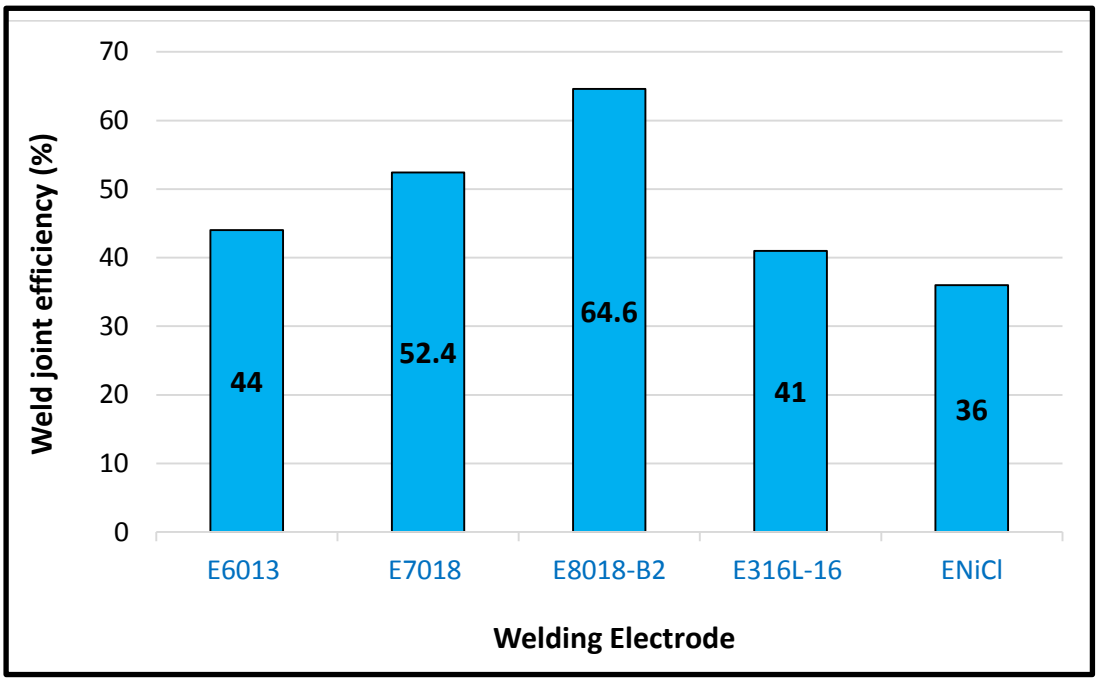

Figure (4.10): The joint efficiency for each weld.

It could be noted from the Figure (4.8) that the average tensile strength value of the weld resulting from the use of the E6013 electrode, which represents the actual tensile strength of the weld metal, was (650MPa). It is higher than the typical tensile strength of the weld metal (510MPa) while using this electrode (Table 3.3). Figure (4.10) shows that the efficiency of this weld joint was relatively low (44%). This might be because the E6013 electrode is specially manufactured for welding mild steel, not for welding low alloy steels, as it is a cellulosic electrode (high in hydrogen), which

exposes hardenable steel welds to welding cracks of both types, hot and cold. The weld tensile strength thus decreases, in addition to causing porosity for being high in hydrogen **[25,45,46]**. E6013 electrode was used in this study for comparison, as it is the cheapest and most common and widespread welding electrode. This is because its cover contains a high percentage of titania and potassium, the materials that ionized easily when heated by the electric arc, thus increases arc stabilility during welding and facilitates ignition **[47]**.

It is also clear from the Figure (4.8) that the tensile strength of the weld resulting from the use of the E7018 welding electrode was (761MPa), which is higher than the typical tensile strength of the weld metal (540MPa) when using this electrode (Table 3.3). The efficiency of this weld was (52.4%) (Figure 4.10), because the electrode wire made of mild steel, not of low alloy steels (Table 3.3). As for the relative increase in the value of tensile strength, it might be due to the electrode cover contains a high percentage of iron powder and low in hydrogen (Table 3.3). This high percentage of iron powder (which may reach 40%), increases the deposition rates, and decreases the dilution ratio, which avoids hot cracks in welds. In addition to being low in hydrogen, which prevents the occurrence of cold cracks, as well as the porosity in the weld metal. The weld metal resulting from the use of this electrode contains approximately (1.1% Mn), which would also increase the tensile strength of the weld metal **[25,45,46,48]**.

While using the E8018-B2 electrode, it is clear from the Figure (4.8) that the tensile strength of the weld has increased to (938MPa), which is higher

than the tensile strength of the weld metal (620MPa) when using this electrode (Table 3.3). Figure (4.10) shows that the efficiency of the weld joint also increased to (64.6%). This might be because the covering of this electrode (designed for welding low alloy steels) contains a high percentage of iron powder and low in hydrogen (Table 3.3), which would avoid weld cracks, both hot and cold, and porosity as well (as mentioned earlier). In addition, the weld metal resulting from the use of this electrode contains (1.3%Cr, 0.5%Mo) (Table 3.3). These alloying elements (as is well known) increase the tensile strength of the weld metal **[1,25]**.

When using the E316L-16 electrode, which is specialized for welding ausenitic stainless steels, the tensile strength value of the weld metal was (603MPa), which is slightly higher than the tensile strength of the weld metal (580MPa) shown in (Table 3.3). This relatively high value was due to the fact that this electrode is made of austenitic stainless steel, and the austenite is a soft phase, which in turn increases the ductility of the weld metal and decreases its hardness, thus avoiding cracks in the weld metal **[25,49]**.

On the other hand, the ENiCI welding electrode is a nickel electrode specialized for welding cast iron, repairing broken parts and joining parts made of steel, copper or nickel with castings. The weld metal obtained from the use of this electrode contains (Ni≥94 wt. %) **[25,50]**. This increases the ductility of the weld metal and decreases its brittleness to a large extent, thereby avoiding the occurrence of cracks in cast iron. Figures (4.8 and 4.10) shows that as this electrode was used for welding low alloy steel, the tensile strength and the weld joint efficiency were (527MPa) and

(36%) respectively. The reason for these relatively low results is that increasing the percentage of nickel by this amount increases the ductility of the weld metal to a very large extent , which leads to a decrease in the yield strength and tensile strength of the weld metal. This is evident in the fracture area shown in Figure (4.11). It is worth noting that the prices of welding electrodes used in this study increase, starting from the E6013 to the ENiCI.

Figure (4.11): Fractography of the shielded metal arc AISI 5155 low alloy steel weld joined by the use of the ENiCI electrode.

CHAPTER FIVE:

CONCLUSIONS &

RECOMMENDATIONS

CHAPTER FIVE: CONCLUSIONS and RECOMMENDATIONS

5.1 Conclusions

The most significant results of joining 6 mm thickness AISI 5155 low alloy steel plates by the SMAW process using different types of electrodes (E6013, E7018, E8018-B2, E316L-16 and ENiCl) can be concluded as follows:

1- The microstructure of the weld metals ranged from pearlite colonies within a ferrite matrix in addition to a needle-like structure (for E6013 and E7018) to an austenitic structure (for E316L-16 and ENiCl) passing through predominantly acicular ferrite and a small amount of pearlite colonies with ferrite at the grain boundaries (for E8018-B2).

2- The coarsest structure in the HAZ was for all welds in the CGHAZ immediately adjacent to the weld zone; where the structure contained ferrite and pearlite coarser than that of the base metal. The finest structure across the welds was however in the intercritical HAZ, where the pearlite might be partially spherodized.

3- The average hardness value of the weld metal, for each weld, was lower than that of the base metal (~465 HV). The maximum hardness across the center of shielded metal arc welds was in the CGHAZ at a small distance away from the weld center, whereas the minimum hardness was in the intercritical HAZ.

4- The highest hardness value of the weld metals was (~337 HV) for the weld resulted from the use of the E7018 electrode, whereas the lowest one was (~239 HV) for the weld achieved using the E6013 welding electrode.

5- The maximum tensile strength and thus joint efficiency were (938 MPa and 64.6% respectively) for the weld resulted from the use of the E8018-B2 electrode, while the minimum values were (527 MPa and 36%) for the weld achieved using the ENiCl electrode.

6. The low cost, commonly used, cellulosic (high hydrogen) welding electrode (E6013), and the expensive electrode (ENiCl) gave relatively poor mechanical properties (hardness and tensile strength) in shielded metal arc AISI 5155 low alloy steel welds. These properties notably increased while using iron powder low hydrogen covering electrodes (E7018 and E8018-B2).

5.2 Recommendations

There are some suggestions that can be taken into consideration for future work:

1. Other welding processes can be used for comparison, such as SAW, TIG and MIG.

2. The impact test can also be carried out for low alloy steel welds to identify their toughness.

3. Using X- ray radiography to detect the size, number, location and type of some internal defects in the welds.

4. The use of the SEM and EDS examinations for more details on micrography.

References

[1] Bailey F. W. J. (1972), *Fundamentals of Engineering Metallurgy and Materials*, 5th ed, London.

[2] Khanna O. P. (1980), *Welding Technology*: A text Book for Engineering Students, Dhanpat Rai and Sons, 1st ed, Delhi.

[3] Levy B. S. (1979), *Design and Manufacturing Guidelines for Ultra High Strength Steel Bumper Reinforcement Beams*, No. 79033 SAE Transactions, 1151-1161.

[4] Fine T. E. and Dinda S. (1975), *Development of Lightweight Door Intrusion Beams Utilizing an Ultra High Strength Steel*, No. 750222 SAE Technical Paper.

[5]https://www.cs.mcgill.ca/~rwest/wikispeedia/wpcd/wp/s/Shielded_metal arc_welding.htm.

[6] Groover M. P. (1997), *Fundamentos de Manufactura Moderna*, México: Prentice hall, pp. 641-645.

[7] https://whatispiping.com/types-of-steel.

[8] Mandal S. K. (2015), *Steel Metallurgy: Properties, Specifications and Applications*, McGraw-Hill Education.

[9] *Steel Grading: Chemistry and Properties* (2018) from: https://www.reliance-foundry.com/blog/steel-grades.

[10] Narula G. K., Narula K. S. and Gupta V. K. (1989), *Materials Science*, Tata McGraw-Hill Education.

[11] Phillips D. H. (2016), *Welding Engineering: An Introduction*, United Kingdom: John Wiley & Sons, Ltd.

[12] Pickering F. B. (1992), *Constitution and Properties of Steels*, Verlag GmbH & Co. KGaA, Weinheim.

[13] Mackenzie S. (2017), *Factors that Affect Hardenability*, Retrieved from Gearsolutions.

[14] Technical committee, Indian institute of Welding, Bangalore branch. (Dec., 1977) *Welding Metallurgy, technology and quality assurance*, Venue: Bangalore.

[15] Amani J. (2011), Effect of Submerged Arc Welding Parameters on the Microstructure of SA516 and A709 Steel Welds.

[16] د. عبد الرزاق اسماعيل خضر ود. نوفل محمد حسين ,(1993) تكنولوجيا اللحام ,الجامعة التكنولوجية.

[17] Kuppan T. (2000), Heat Exchanger Design Handbook, Marcel Dekker, Inc.

[18] د.قحطان خلف الخزرجي و عبد الجواد محمد محمد احمد الشريف (1988) ،تكنلوجيا اللحام, جامعة بغداد.

[19] https://uotechnology.edu.iq/dep-production/lectures/WL.pdf.

[20] William L. and Ballis, P. E. (2010), *Shielded Metal Arc Welding Theories and Techniques*.

[21] Jung K. H. (2018), *Shielded Metal Arc Welding*, Ph.D. thesis.

[22] Khan M. I. (2007), *Welding Science and Technology*, New Age International (P) Ltd.

[23] Finch R. (2005), *The Farm Welding Handbook.*

[24] Lee F. (1809), *WELDING OPERATIONS, I SUBCOURSE OD1651 EDITION 8,* Army Institute for Professional Development.

[25] ESAB (2001), *Consumable for Manual and Automatic Welding*, Welding Handbook, 6th ed.

[26]https://www.fabtechexpo.com/blog/2018/01/04/shielded-metal-arc-welding-basics.

[27] Galvery W. and Marlow F. (2000), *Welding essentials*, industrial press, Inc.

[28] Brumbaugh J. E. and Miller R. (2007), *Welding Pocket Reference*, Canada: Wiley Publishing, Inc.

[29] Syahroni N., Rochani I. and Nizar H. (2006), *EXPERIMENTAL STUDY OF ELECTRODE SELECTION EFFECTS ON MECHANICAL PROPERTIES OF UNDERWATER WET WELDED-JOINTS*.

[30] Verma J., Taiwade R. V., Khatirkar R. K. and Kumar A. (2016), *A comparative study on the effect of electrode on microstructure and mechanical properties of dissimilar welds of 2205 austeno-ferritic and 316L austenitic stainless steel*, Materials Transactions, 57(4), pp.494-500.

[31] Tahir A. M., Lair N. A. M. and Wei F. J. (2018), *Investigation on mechanical properties of welded material under different types of welding filler (shielded metal arc welding)*, In AIP conference proceedings (Vol. 1958, No. 1, p. 020003). AIP Publishing LLC.

[32] Winarto W., Purnama D. and Churniawan I. (2018), *The effect of different rutile electrodes on mechanical properties of underwater wet welded AH-36 steel plates*, In AIP Conference Proceedings (Vol. 1945, No. 1, p. 020048). AIP Publishing LLC.

[33] Nassar A., Lefta R. and Abdulsada M. (2018), *Experimental Study of The Effect of Welding Electrode Types on Tensile Properties of Low Carbon Steel Aisi1010*, Kufa Journal of Engineering, 9(4), pp.163-173.

[34] Sumardiyanto D., Susilowati S. E. (2019), *Effect of Welding Parameters on Mechanical Properties of Low Carbon Steel API 5L*

Shielded Metal Arc Welds, American Journal of Materials Science, Vol. 9 No. 1,pp. 15-21.

[35] Pratomo M. A., Jasman J., Erizon N. and Fernanda Y. (2020), *The Variation Effect of Electric Current Toward Tensile Strength on Low Carbon Steel Welding with Electrode E7018*, Teknomekanik, 3(1), pp.9-16.

[36] Manesh T. H. and Nasresfahani A. (2021), *Evaluation of microstructural properties and investigation of corrosion behavior of P460NH welded steel using E8018-G electrode*, Journal of Welding Science and Technology of Iran, 7(1), pp.89-100.

[37] Yousaf A., Pasha R. A. and Muhammad A. (2021), *Effect of Filler Materials on Mechanical Properties of Shielded Metal Arc Welded AISI 316L Austenitic Stainless-Steel Joints*.

[38] Spring Steels AISI AISI-5155 | Steel Database Query Result | Ju Feng Special Steel Co., Ltd. (jfs-steel.com).

[39]http://www.matweb.com/search/datasheet.aspx?matguid=275c6729d8444064b147a663eb2824a1&ckck=1.

[40] Technical committee (1977), *Welding Metallurgy, technology and quality assurance*, Indian institute of Welding, Bangalore branch Venue: Bangalore.

[41] Hammadi D. K. Y. (2021), *The Effect of Nickel Additions on Submerged Arc Low Alloy Steel Weld*.

[42] Trindade V. B., Payão J. D. C., Souza L. F. G. and Paranhos R. D. R. (2007), *The role of addition of Ni on the microstructure and mechanical behavior of C-Mn weld metals*, Exacta, São Paulo, v. 5, n. 1, p. 177-183.

[43] Gomes M. D. G. M. D. F., De Almeida L. H., Gomes L. C. F.C. and Le May I. (1997), *Effects of Microstructural Parameters on the Mechanical Properties of Eutectoid Rail Steels*, Materials Characterization, 39(1):1-14.

[44] Lancaster J. F. (1987), *Metallurgy of Welding*, 14th ed Allen and Unwin, London.

[45] Gray T. G. F. (1982), *Rational Welding Design*.

[46] Stuart W. G. (1997), *Advanced Welding*.

[47] ASM, Metals Handbook (1971), *Welding and Brazing*, 8th ed.

[48] Sacks R. (1981), *Welding: Principles and Practices*.

[49] ASM, Metals Handbook (1975), *Failure Analysis and Prevention*, 18th ed.

[50] Oerlikon (2002), *Handbook of Welding Consumables*, COBISA GmbH Germany.

ملخص البحث

تم استخدام الفولاذ منخفض السبائك في الصناعات الهندسية إلى حد كبير، حيث يمتلك العديد من التطبيقات االمهمة في تصنيع الآلات الزراعية وأنابيب النفط والغاز وكذلك المعدات الصناعية والتي من المحتمل أن تفشل أثناء الخدمة مما يتطلب إصلاحها بإحدى عمليات اللحام. من ناحية أخرى، يعتبر لحام القوس الكهربائي المعدني المغلف أكثر عمليات اللحام شيوعًا وانتشارًا. تهدف الدراسة إلى بحث ومقارنة الخواص الميكانيكية (الشد والصلادة) والبنية المجهرية الناتجة عن استخدام أقطاب لحام مختلفة (E6013, E7018, E8018-B2, E316L-16, ENiCl) للحام ألواح بسمك 6 مم من الفولاذ منخفض السبائك (AISI 5155) بطريقة القوس الكهربائي المعدني المغلف. أظهرت النتائج أن بنى معادن اللحام تنوعت بين مستعمرات برلايتية داخل ارضية من الفريت بالإضافة إلى بنية إبرية الشكل (لاقطاب اللحام E6013 و E7018) و بنية أوستنايتية (لاقطاب اللحام E316L-16 و ENiCl) مرورا ببنية مكونة بشكل أساس من الفريت الابري مع كمية صغيرة من مستعمرات البرلايت و فرايت عند حدود الحبيبات (لقطب اللحام E8018-B2). كانت البنية المجهرية الأكثر خشونة في HAZولجميع اللحامات هي في CGHAZ، والتي ظهرت فيها أقصى صلادة عبر مراكز الملحومات، حيث احتوت البنية على فريت وبرليت أكثر خشونة مما هي عليه في المعدن الأساس. وكانت البنية الانعم عبر مراكز اللحام هي في ICHAZ، والتي ظهرت فيها أدنى صلادة، حيث قد يكون البرليت فيها قد تكور جزئيًا. كان متوسط قيمة صلادة معدن اللحام، ولجميع الملحومات، أقل مما هو عليه للمعدن الأساس (465 HV~)، حيث كانت أعلى قيمة (337 HV~) هي في معدن اللحام الناتج عن استخدام قطب اللحام E7018، بينما كانت أقل قيمة (239 HV~) هي في اللحام الناتج عن استخدام القطب E6013. كانت أقصى مقاومة شد وبالتالي أعلى كفاءة لوصلة اللحام (938 MPa و 64.6% على التوالي) هي للحام الناتج عن استخدام قطب اللحام E8018-B2، بينما كانت القيم الدنيا (527 MPa و 36%) هي في اللحام الناتج عن استخدام القطب ENiCl. أعطى قطب اللحام المنخفض الكلفة (E6013) والقطب الغالي الثمن (ENiCl) خواص ميكانيكية منخفضة نسبيًا، بينما تحققت الخواص الامثل نتيجة لاستخدام أقطاب اللحام ذات التغطية المحتوية على مسحوق الحديد و المنخفضة الهيدروجين (E8018-B2 , E7018).

وزارة التعليم العالي والبحث العلمي
جامعة بابل
كلية هندسة المواد
قسم هندسة المعادن

دراسة تأثير نوع قطب اللحام على البنية المجهرية والخواص الميكانيكية لملحومات الصلب الواطئ السبائك AISI 5155 بطريقة القوس الكهربائي المعدني المغلف

رسالة

مقدمة الى قسم هندسة المعادن في كلية هندسة المواد/جامعة بابل وهي جزء من متطلبات نيل درجة الدبلوم العالي في هندسة المواد/ المعادن

من قبل

نور عبد علي كاظم عبد

بإشراف

أ. م.د. عبد السميع جاسم عبد الزهرة الكلابي

2021م **1442هـ**